ANALYSIS OF INCIPIENT FAULT SIGNATURES IN INDUCTIVE LOADS ENERGIZED BY A COMMON VOLTAGE BUS

A Thesis

by

RAJESH KUMAR BADE

Submitted to the Office of Graduate Studies of
Texas A&M University
in partial fulfillment of the requirements for the degree of

MASTER OF SCIENCE

December 2004

Major Subject: Mechanical Engineering

ANALYSIS OF INCIPIENT FAULT SIGNATURES IN INDUCTIVE LOADS ENERGIZED BY A COMMON VOLTAGE BUS

A Thesis

by

RAJESH KUMAR BADE

Submitted to Texas A&M University
in partial fulfillment of the requirements
for the degree of

MASTER OF SCIENCE

Approved as to style and content by:

Alexander G. Parlos (Chair of Committee)	Won-jong Kim (Member)
Mahboobul Mannan (Member)	Dennis L. O'Neal (Head of Department)

December 2004

Major Subject: Mechanical Engineering

ABSTRACT

Analysis of Incipient Fault Signatures in Inductive Loads
Energized by a Common Voltage Bus.
(December 2004)
Rajesh Kumar Bade, B.E., Osmania University, Hyderabad, India
Chair of Advisory Committee: Dr. Alexander G. Parlos

Recent research has demonstrated the use of electrical signature analysis (ESA), that is, the use of induction motor currents and voltages, for early detection of motor faults in the form of embedded algorithms. In the event of multiple motors energized by a common voltage bus, the cost of installing and maintaining fault monitoring and detection devices on each motor may be avoided, by using bus level aggregate electrical measurements to assess the health of the entire population of motors. In this research an approach for detecting commonly encountered induction motor mechanical faults from bus level aggregate electrical measurements is investigated.

A mechanical fault indicator is computed processing the raw electrical measurements through a series of signal processing algorithms. Inference of an incipient fault is made by the percentage relative change of the fault indicator from the "healthy" baseline, thus defining a Fault Indicator Change (FIC).

To investigate the posed research problem, healthy and faulty motors with broken rotor bar faults are simulated using a detailed transient motor model. The FIC based on aggregate electrical measurements is studied through simulations of different motor banks containing the same faulty motor. The degradation in the FIC when using aggregate measurements, as compared to using individual motor measurements, is investigated. For a given motor bank configuration, the variation in FIC with

increasing number of faulty motors is also studied. In addition to simulation studies experimental results from a two-motor setup are analyzed. The FIC and degradation in the FIC in the case of load eccentricity fault, and a combination of shaft looseness and bearing damage is studied through staged fault experiments in the laboratory setup.

In this research, the viability of using bus level aggregate electrical measurements for detecting incipient faults in motors energized by a common voltage bus is demonstrated. The proposed approach is limited in that as the power rating fraction of faulty motors to healthy motors in a given configuration decreases, it becomes far more difficult to detect the presence of incipient faults at very early stages.

To My Parents

ACKNOWLEDGMENTS

I would like to convey my sincere gratitude to my committee chair and advisor, Dr. Alexander G. Parlos, for his continuous guidance and support during the course of this work. I also thank Dr. Won-jong Kim and Dr. Mahboobul Mannan, for their time and interest in my research.

Finally, I would like to acknowledge and thank, all the students at NIML, especially, Aninda and Parasuram, for several insightful discussions on related and unrelated topics, alike.

TABLE OF CONTENTS

CHAPTER Page

CHAPTER Page

LIST OF TABLES

LIST OF FIGURES

FIGURE Page

FIGURE Page

FIGURE Page

FIGURE Page

CHAPTER I

INTRODUCTION

A. Motivation

Induction motors form the majority of electrical motors in contemporary industries. Failure of such motors results in severe loss of productivity. Several diagnostic methodologies have been adopted to keep the up-time of these machines to a maximum. The existing techniques of preventive and periodic maintenance may lead to undesirable replacement of healthy parts in addition to unavoidable downtime. The concept of on-line "health" monitoring and "health" assessment helps circumvent this problem. This involves monitoring the health of a motor continuously, through a set of signals, corresponding to vibration and/or electrical measurements of a motor and then assessing its "health". Apart from their lower reliability, costs associated with acquisition, installation and maintenance of accelerometers used in vibration monitoring is often considered prohibitive. Thus, "sensor-less" motor fault diagnosis using electrical currents and voltages, presents itself as a viable option. These electrical signals could be obtained from standard installations in a typical industrial setup, with minimal capital investment.

In practice, several induction motors are energized from a common voltage bus for operational convenience. The detection of motor faults using bus level aggregate information allows an opportunity to reduce costs associated with having monitoring devices on each motor. In this context, the feasibility of detecting faults in a bank of multiple induction motors using "aggregate" bus voltages and currents, assumes importance. Figure 1 depicts the conventional and proposed arrangements of monitoring

---

The journal model is *IEEE Transactions on Automatic Control.*

devices for a group of induction motors.

B. Terminology

Henceforth, a motor under normal operating conditions will be termed as a "healthy" motor and one with an incipient fault as a "faulty" motor. A set of motors energized by a common voltage bus, will be termed as a "motor bank". A motor bank with a specified number and power rating of motors, will be a "configuration". A faulty configuration need not have all faulty motors. The term, "aggregate" currents, will be used to indicate the bus currents. A "fault indicator" will be a fault measure arrived at, after requisite processing of the electrical signals, to adequately reflect the health of a motor or a configuration. Inference of an incipient fault is made by the percentage relative change of the fault indicator from the healthy baseline, termed as 'Fault Indicator Change' (FIC).

C. Mechanical Faults in Induction Motors

Faults in induction motors can be broadly classified into electrical faults and mechanical faults. Electrical faults include excessive power supply imbalance, stator winding shorts, while mechanical faults include bearing defects and rotor faults. According to some motor reliability surveys [1], about 80% of induction motor failures are caused due to problems with three components viz., stator, rotor and bearings. A brief overview of the different forms of mechanical faults follows.

Despite the rugged architecture of the squirrel-cage construction, rotor faults occur in induction motors. Startup transients and high centrifugal forces created by load fluctuations propagate a defect once it is initiated. While mechanical signature monitoring promises to be an easy detection method for such faults, methods have

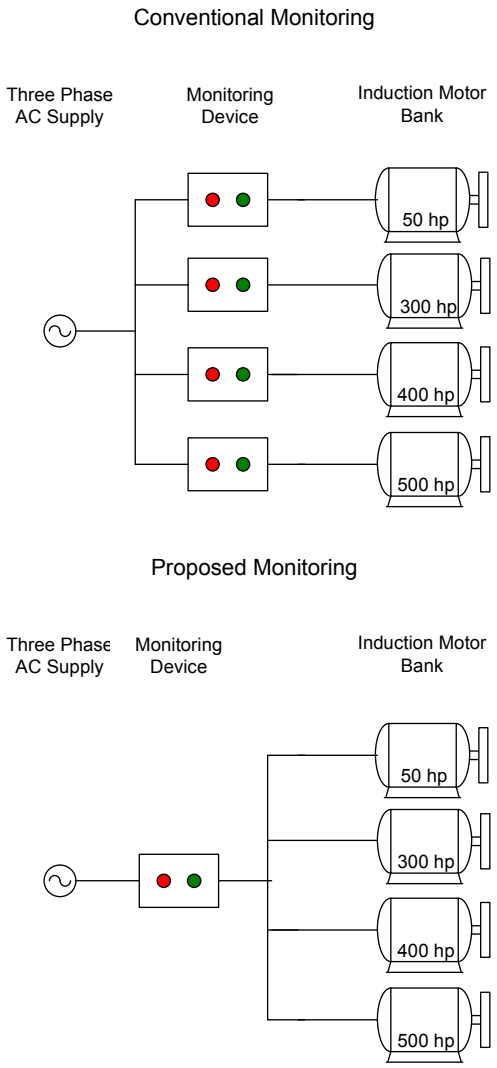

Fig. 1. Conventional monitoring and proposed monitoring of a group of induction motors energized by a common voltage bus.

also been developed using frequency component monitoring of the current spectrum associated with broken rotor bars. Rolling element bearings are the most common type of bearings used to provide rotor support in induction motors. Localized fatigue caused due to continual stresses, improper lubrication, corrosion and improper installation are a few modes through which bearing faults may occur. Air-gap eccentricity is another mechanical fault type, and it can be classified into static and dynamic air-gap eccentricity. When positioning of the stator or the rotor is incorrect or when there is an ovality of the core, static air-gap eccentricity is caused. Dynamic air-gap eccentricity can be caused by bearing wear, bearing misalignment, bent rotor shaft etc. Both types of eccentricities can cause a lot of damage to the bearings, core, windings and the rotor cage. Not integral with motor, but nevertheless considered a fault, is the eccentricity of the load. Such faults are caused due to improper commissioning of load.

D. Fault Detection in Induction Motors

Several methods have been proposed to detect and diagnose incipient motor faults. These include both electrical faults and mechanical faults. This work will consider only mechanical faults. Payne et al. [2, 3] performed an investigation into detection and diagnosis of broken rotor bars by the use of vibration and phase current analysis. Emphasis was given to demonstrating higher potential with the use of current spectra. Elkasabgy et al. [4] demonstrated that the detection of a broken bar could actually be carried out in three distinct ways: a) Motor Current Signature Analysis (MCSA), which involves frequency analysis of the stator current for monitoring frequency components associated with faults; b) Use of internal or external search coils to measure variations in the magnetic flux density as a function of time; c) Monitoring

the twice-slip frequency components induced in the motor torque.

Schoen et al. [5] addressed the application of motor current spectral analysis for the detection of rolling element bearing damage in induction motors. Yazici et al. [6] developed a statistical time-frequency based method for detecting bearing damage and broken rotor bars. They used an algorithm that is trained to recognize healthy operating condition, and flag new operating modes, thus indicating the presence of faults. Thomson et al. [7] were able to successfully demonstrate the identification of faults in the motor spectral components.

Kim [8, 9], presents an alternative approach to MCSA by using the overall distortion of the stator current as an indicator for the presence of a fault. This approach has the advantage of being insensitive to uncertainty in the frequencies at which faults appear in the current spectrum. Benbouzid et al. [10] demonstrated the use of stator current processing for the detection and localization of faults in an induction motor.

Also, Benbouzid [11] provides a tutorial overview of induction motor fault diagnosis by the use of motor signature analysis, while reference [12] focuses on providing a detailed bibliography of all relevant previous work toward induction motor fault detection and diagnosis.

E. Literature Review

Little literature exists, which exploit the idea of using aggregate current and voltage measurements, for "health" assessment of motor banks and/or their loads. Considerable work has been done in Non-intrusive Appliance Load Monitoring (NALM) [13, 14, 15, 16], as applied to residential and industrial setups. NALM involves using aggregate signals obtained from bus measurements to assess the sequence and nature of operation of various loads in the setup. It exploits information-rich transients in

power, both reactive and real, associated with start-ups and shutdowns of different loads. It is based on the "uniqueness" of loads in a setup and principally offers monitoring the status of operation rather than fault detection of parallel loads. Another NALM approach proposed by Shaw [17], uses spectral envelopes of the aggregate currents. Estimation of damping and inertia parameters is employed as a means for fault detection in the driven loads.

Another related area of work is the vector control of an induction motor bank, through a single inverter source [18]. Motor banks with identical motors have been modeled, assuming balanced three-phase operation, for speed control [19].

F. Research Objectives, Proposed Approach and Assumptions

1. Objectives

The incentive of a centralized diagnostic system for a motor bank, as opposed to having instrumentation on each motor, drives the need for this work. The principal aim of this research is to study the detectablity of various mechanical faults in induction motors energized by a common voltage bus, using aggregate bus-level current signals. Faults considered are broken rotor bars, bearing damage with rotor looseness and load eccentricity. It is aimed to study, how Fault Indicator Change degrades as the number of healthy motors in the motor bank, increase. Variation in Fault Indicator Change with increasing number of faulty motors in a fixed configuration, will also be studied.

2. Proposed Approach

The relative difference in motor fault indicator corresponding to healthy and faulty configurations, forms the basis of fault detection. On-line diagnostic methods use

empirical models like neural networks [9], to compute fault indicators for healthy configurations. The proposed study will be carried out off-line and currents corresponding to both healthy and faulty configurations will be obtained alike.

Part of the study will be carried out using simulations of healthy and faulty motors. The simulation model of induction motors used is capable of modeling fault conditions like broken rotor bar, stator winding short, static and dynamic eccentricity. The simulator is based on the motor model proposed in [20]. Currents obtained from various simulations, will be summed, to obtain aggregate bus currents. A fault indicator capable of reflecting the health of the motor configuration, will be chosen, whilst exploiting the advantages of analyzing the electrical measurements. The relative difference in the indicator between a faulty and a healthy configuration (known *a priori*) gives a measure of the health of the setup. The simulation model will be used to study broken rotor bar faults.

The effectiveness of the approach to other mechanical faults, viz., bearing damage with rotor looseness and load eccentricity, will be demonstrated through staged fault experiments in a laboratory setup. Statistical consistency will be verified through multiple data sets of a given configuration.

3. Assumptions

The desired analysis will be performed under following operational assumptions:

- The configuration is part of an infinite voltage bus,
- All the motors are at steady–state loading conditions,
- Power supply quality is not varying,
- All healthy motors are at same load level,

- All faulty motors are at same load level, and,
- All faulty motors have same fault type and same fault severity.[1]

G. Potential Contributions

Following are some key anticipated contributions of this research towards induction motor condition assessment:

1. Analysis of incipient mechanical fault signatures to demonstrate the feasibility of using bus-level aggregate electrical measurements for fault detection in induction motors energized by a common voltage bus.
2. Demonstration of applicability of the proposed approach to mechanical faults of different nature and motors of different power rating.

H. Organization of the Thesis

The rest of the thesis report is organized as follows. The theory of modeling an induction motor under healthy and faulty operating conditions is described in Chapter II. Chapter III presents the procedural steps involved in obtaining the fault indicator from raw current signals. In Chapter IV, the simulations performed are described. Different quantities used for presenting the results are defined. Two problems are defined for the study of variation of Fault Indicator Change in simulated motor banks. In Chapter V, the experimental setup and the experiments conducted are described. The adaptability of the indicator to different mechanical faults and their detectability from aggregate currents is demonstrated.

---

[1]Does not apply to the faults staged in the laboratory setup

CHAPTER II

MODELING HEALTHY AND FAULTY INDUCTION MOTORS

The simulator used in this work is based on the analysis of squirrel-cage induction machines under healthy operating conditions and rotor asymmetries [20]. A portion of the theory developed in the cited reference is reproduced in the following section for completeness.

A. Modeling an Induction Machine with m Stator Phases and n Rotor Bars

Consider a general m–n winding machine (m stator phase windings and n rotor bars) with the following assumptions:

- negligible saturation,
- m identical stator windings with axes of symmetry,
- n uniformly distributed cage bars with axes of symmetry,
- negligible eddy current and windage losses, and,
- insulated rotor bars.

A squirrel cage rotor can be modeled using n identical and equally spaced rotor loops, as depicted in Figure 2. In a cage with n bars, there are $2n$ nodes and $3n$ branches. Therefore, rotor current distribution can be specified in terms of $n + 1$ independent rotor currents comprising of n rotor loop currents (i_k^r, $1 \leq k \leq n$) and an end ring current (i_e). The rotor loop currents are coupled to each other and to the stator windings through mutual inductances. The end ring loop current couples only with rotor loops through the end ring leakage inductance and the end ring resistance.

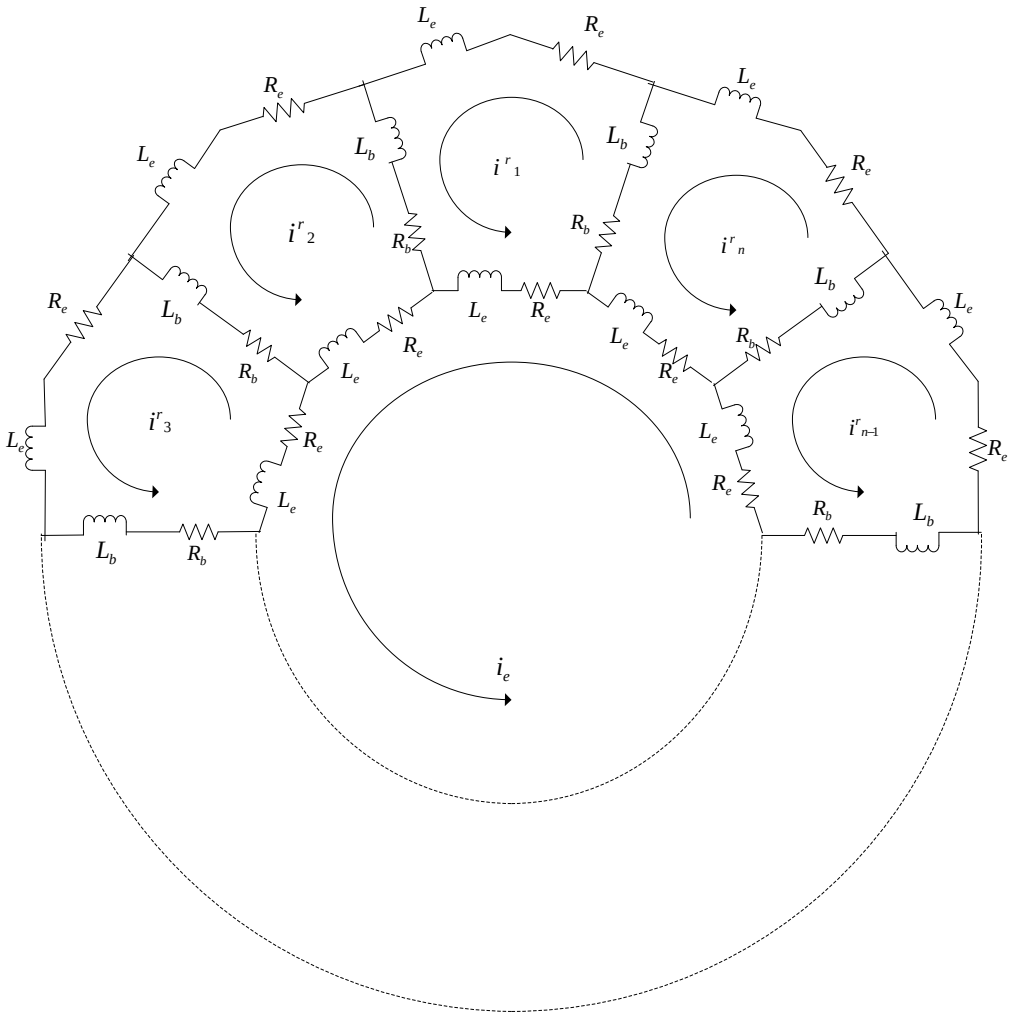

Fig. 2. Equivalent circuit of a healthy squirrel cage rotor with rotor loop currents and end ring current.

1. Stator Voltage Equations

The voltage equations for the stator loops can be written as,

$$V_s = R_s I_s + \frac{d\Lambda_s}{dt}, \tag{2.1}$$

where,

$$\begin{aligned}
\Lambda_s &= L_{ss} I_s + L_{sr} I_r, \\
I_s &= \left[i_1^s \; i_2^s \; \ldots \; i_m^s \right]^T, \\
I_r &= \left[i_1^r \; i_2^r \; \ldots \; i_n^r \; i_e \right]^T, \\
V_s &= \left[v_1^s \; v_2^s \; \ldots \; v_m^s \right]^T,
\end{aligned}$$

where Λ_s is the stator flux linkage, R_s is an m by m diagonal matrix of resistances of each stator coil. The matrix L_{ss} is a symmetric m by m matrix. Since there is no relative motion between the stator coils, the elements of L_{ss} are constant. The mutual inductance matrix L_{sr} is an m by n matrix consisting of mutual inductances between stator coils and the rotor loops, as follows:

$$L_{sr} = \begin{bmatrix}
L_{11}^{sr} & L_{12}^{sr} & \ldots & L_{1n}^{sr} & L_{1e}^{sr} \\
L_{21}^{sr} & L_{22}^{sr} & \ldots & L_{2n}^{sr} & L_{2e}^{sr} \\
\vdots & \vdots & \ddots & \vdots & \vdots \\
L_{m1}^{sr} & L_{m2}^{sr} & \ldots & L_{mn}^{sr} & L_{me}^{sr}
\end{bmatrix}.$$

The second term of the Equation (2.1) can be expressed as,

$$\frac{d\Lambda_s}{dt} = L_{ss}\frac{dI_s}{dt} + \omega_{rm}\frac{dL_{sr}}{d\theta_{rm}} + L_{sr}\frac{dI_r}{dt} \tag{2.2}$$

where, θ_{rm} is the angular position of the rotor and ω_{rm} is the mechanical speed.

2. Rotor Voltage Equations

The voltage equations for the rotor loops can be written, from Figure 2, as,

$$V_r = R_r I_r + \frac{d\Lambda_r}{dt}, \tag{2.3}$$

where,

$$\begin{aligned} V_r &= [v_1^r \; v_2^r \; \ldots \; v_n^r \; v_e]^T, \\ \Lambda_r &= L_{rs} I_s + L_{rr} I_r, \end{aligned}$$

where Λ_r is the rotor flux linkage, L_{rs} is the mutual inductance from rotor loops to the stator coils and is the transpose of the matrix L_{sr}. The matrix R_r is the $n+1$ by $n+1$ symmetric matrix, as shown below, where R_e is the end ring resistance and R_b is the rotor bar resistance. In matrix L_{rr}, L_{mr} is the magnetizing inductance of each rotor loop, L_b the rotor bar leakage inductance, L_e the rotor end ring leakage inductance and $L_{r_i r_j}$ the mutual inductance between two rotor loops i and j. In case of a squirrel cage rotor, the end ring voltage, v_e, and rotor loop voltages, $v_k^r (1 \leq k \leq n)$, are equal to zero.

$$R_r = \begin{bmatrix} 2(R_b+R_e) & -R_b & 0 & \ldots & 0 & -R_b & -R_e \\ -R_b & 2(R_b+R_e) & -R_b & \ldots & 0 & 0 & -R_e \\ \vdots & \vdots & \vdots & \ddots & \vdots & \vdots & \vdots \\ 0 & 0 & 0 & \ldots & 2(R_b+R_e) & -R_b & -R_e \\ -R_b & 0 & 0 & \ldots & -R_b & 2(R_b+R_e) & -R_e \\ -R_e & -R_e & -R_e & \ldots & -R_e & -R_e & nR_e \end{bmatrix}$$

$$L_{rr} = \begin{bmatrix} L_{mr}+2(L_b+L_e) & L_{r_1r_2}-L_b & ... & L_{r_1r_{n-1}} & L_{r_1r_n} & -L_e \\ L_{r_2r_1}-L_b & L_{mr}+2(L_b+L_e) & ... & L_{r_2r_{n-1}} & L_{r_2r_n} & -L_e \\ \vdots & \vdots & \ddots & \vdots & \vdots & \vdots \\ L_{r_{n-1}r_1} & L_{r_{n-1}r_2} & ... & L_{mr}+2(L_b+L_e) & L_{r_{n-1}r_n} & -L_e \\ L_{r_nr_1}-L_b & L_{r_nr_2} & ... & L_{r_nr_{n-1}} & L_{mr}+2(L_b+L_e) & -L_e \\ -L_e & -L_e & ... & -L_e & -L_e & nL_e \end{bmatrix}$$

3. Calculation of Torque

The torque generated by the motor is opposed by the inertial torque, the external load torque and the torques due to stiffness and damping of the machine system. A simple mechanical equation of motion is,

$$J\frac{d^2\theta_{rm}}{dt^2} + c\frac{d\theta_{rm}}{dt} + k\theta_{rm} + T_L = T_e \tag{2.4}$$

where, T_e is the electromagnetic torque, T_L is the load torque, c and k are the damping and the stiffness constants of the motor, respectively. The electrical torque can be obtained from the magnetic coenergy W_{co} as,

$$T_e = \left[\frac{\delta W_{co}}{\delta\theta_{rm}}\right]_{(I_s, I_r constant)}. \tag{2.5}$$

In a linear magnetic system the coenergy is equal to the stored magnetic energy,

$$W_{co} = \frac{1}{2}I_s^T L_{ss} I_s + \frac{1}{2}I_s^T L_{sr} I_r + \frac{1}{2}I_r^T L_{rs} I_s + \frac{1}{2}I_r^T L_{rr} I_r. \tag{2.6}$$

Since L_{rr} and L_{ss} contain constant elements, Equation (2.5) reduces to,

$$T_e = \frac{1}{2}I_s^T \frac{\delta L_{sr}}{\delta t} I_r + \frac{1}{2}I_r^T \frac{\delta L_{rs}}{\delta t} I_s. \tag{2.7}$$

4. Calculation of Inductances

From winding function theory, according to [21], the mutual inductances between any two windings i and j in an electric machine are given by,

$$L_{ij}(\theta_{rm}) = \mu_0 \ell \int_0^{2\pi} r(\theta_r, \phi)\, g^{-1}(\theta_r, \phi)\, n_i(\theta_r, \phi)\, N_j(\theta_r, \phi)\, d\phi, \tag{2.8}$$

$$L_{ji}(\theta_{rm}) = \mu_0 \ell \int_0^{2\pi} r(\theta_r, \phi)\, g^{-1}(\theta_r, \phi)\, n_j(\theta_r, \phi)\, N_i(\theta_r, \phi)\, d\phi, \tag{2.9}$$

where θ_{rm} is the angular position of the rotor with respect to some stator reference, ϕ is a particular position along stator inner surface, $g^{-1}(\theta_r, \phi)$ is termed the inverse gap function, ℓ is the length of the stack and r is the average radius of the air-gap. The term $n_i(\theta_r, \phi)$ is the winding distribution of winding i and $N_j(\theta_r, \phi)$ is the winding function of winding j.

The relevant inductances can be calculated using the winding function method proposed in [22]. A demonstration of this method for calculation of inductances of a three phase, two pole induction machine with concentrated windings, is presented in [23].

5. Modeling Broken Rotor Bar Fault

The equivalent circuit of the rotor with a broken bar between rotor loops $n-1$ and n is depicted in Figure 3. The loop current i^r_{n-1} is flowing in a double width rotor loop compared to the same in Figure 2. This condition is incorporated in the inductance matrix L_{rr} by merging the two columns n and $n-1$ into one, by addition. The corresponding rows are also merged into one and replaced by their sum. Similar operations are carried out on the resistance matrix, R_r. For inductance matrices L_{sr} and L_{rs}, the transformation is applied on corresponding columns and rows, respectively. In the case of additional broken rotor bars, the reduction process

is repeated, accordingly.

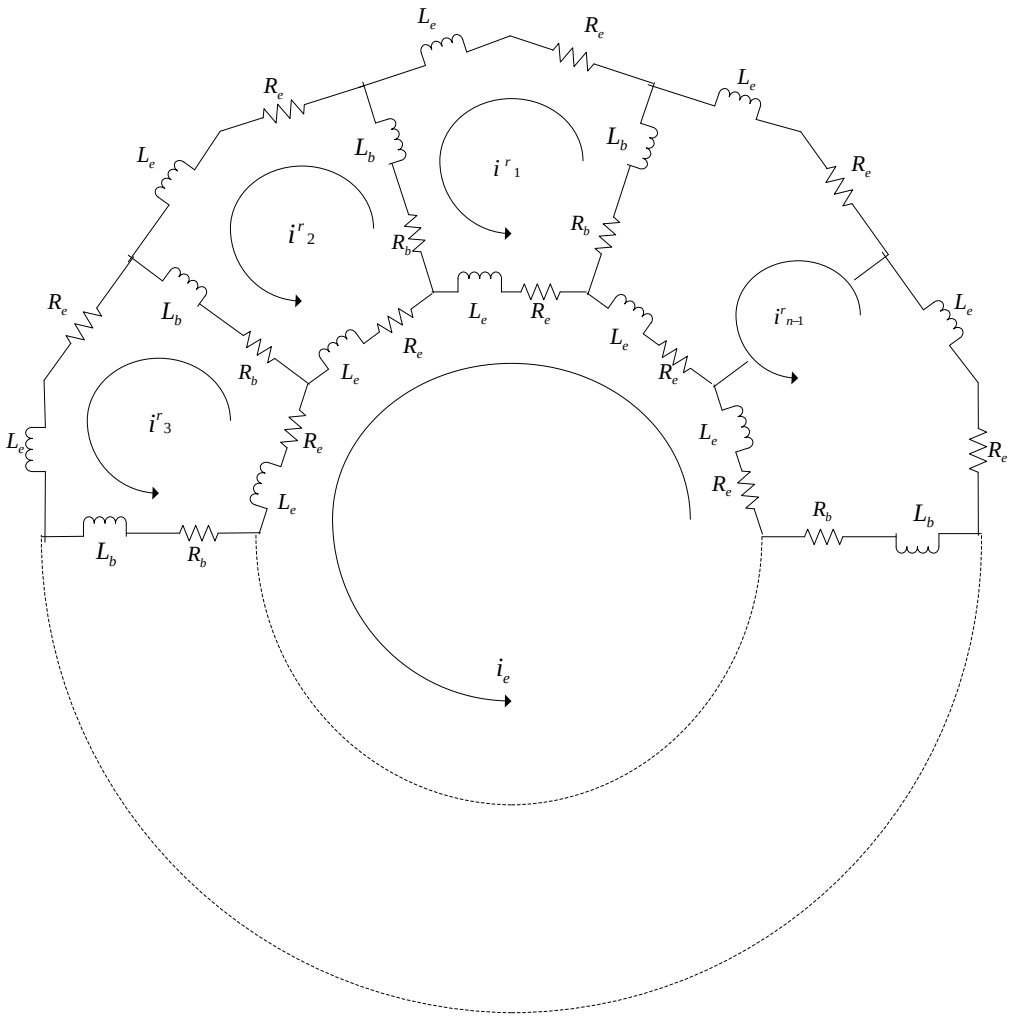

Fig. 3. Equivalent circuit of a squirrel cage rotor with a broken rotor bar fault.

B. State Space Model

For simulating the model presented in the previous section, the equations (2.1), (2.3), (2.4) and (2.7), after rearrangement, can be expressed in the following non–linear state–space form:

$$E(x)\,\dot{x} = f(x) + u \tag{2.10}$$

$$y = h(x) \tag{2.11}$$

where, x is the state vector, u is the forcing function, y is the output vector, $E(x)$ is the "mass" matrix, $f(x)$ and $h(x)$ are non-linear functions of the state vector, defined as follows:

$$\begin{aligned}
x &= [I_s\ I_r\ \theta_{rm}\ \omega_{rm}]^T, \\
u &= [V_s\ V_r\ 0\ -T_L]^T, \\
y &= [I_s\ \omega_{rm}\ T_e]^T, \\
E(x) &= \begin{bmatrix} L_{ss} & L_{sr} & 0 & 0 \\ L_{rs} & L_{rr} & 0 & 0 \\ 0 & 0 & 1 & 0 \\ 0 & 0 & 0 & J \end{bmatrix}, \\
f(x) &= \begin{bmatrix} -R_s I_s - \omega_{rm}\frac{dL_{sr}}{d\theta_{rm}} I_r \\ -\omega_{rm}\frac{dL_{rs}}{d\theta_{rm}} I_s - R_r I_r \\ \omega_{rm} \\ \frac{1}{2}\left(I_s^T L_{sr} I_r + I_r^T L_{rs} I_s\right) - c\omega_{rm} - k\theta_{rm} \end{bmatrix}, \\
h(x) &= \begin{bmatrix} I_s \\ \omega_{rm} \\ \frac{1}{2}\left(I_s^T L_{sr} I_r + I_r^T L_{rs} I_s\right) - c\omega_{rm} - k\theta_{rm} \end{bmatrix},
\end{aligned}$$

Thus, for an applied stator voltage and external load, the stator currents, the rotor speed and the electrical torque can be obtained by solving the simultaneous

differential equations of the aforementioned state–space model.

C. Chapter Summary

The theory of modeling an induction motor using winding function theory, is presented in this chapter. Modeling of broken rotor bars using the simulator is demonstrated. The state–space model on which the simulator used in this work is based, is also presented.

CHAPTER III

INDICATOR DEVELOPMENT

A. Fault Detection Methods and the Signal Processing Approach

Development of an effective fault detection scheme is based on evolving a method to characterize or quantify the normal operating condition of a motor and identify deviatory behavior as a fault. Such methods could be broadly classified into three groups, viz., model-based, knowledge-based and data driven methods. Model-based techniques are based on hardware or analytical replication of the system being monitored. Models capable of, either, replicating the normal behavior of the system in question or estimating parameters and/or states representative of the condition of the motor, form the basis of this method. Model-based methods are generally associated with computationally intensive algorithms. Knowledge-based techniques can be excellent tools for capturing and utilizing knowledge that cannot be captured by models. They are based on applying specific rules to logical interactions between observed symptoms (effects) and unknown faults (causes). They generally work well when a model is not known, or is too complex to develop. But knowledge-based systems suffer from the drawback of requiring extensive reworking in case of a change in the system. A thorough treatment of this subject could be found in [8].

In case of rotating electrical machinery, information contained in electrical and mechanical signals can be utilized for fault detection. Data-driven methods (also known as signal-based methods) use the data collected during normal operating conditions and during specific faults, to develop the fault indicators for detecting faults. Figure 4 shows a signal processing approach to fault diagnosis. Classically, vibration measurements have been used, but lately utilization of electrical signals has attracted

considerable attention. Electrical faults in induction motors are manifested in the form of imbalance in the currents. Common mechanical faults like broken rotor bars, bearing damage, static and dynamic eccentricity, cause variations in air-gap permeance and/or air-gap flux density and thus, ultimately, get reflected in currents. Most of the mechanical faults are associated with sidebands or spikes at characteristic frequencies in motor current spectra and vibration spectra as well [11]. Motor Current Signature Analysis (MCSA) deals with identifying these characteristic frequencies in motor current measurements.

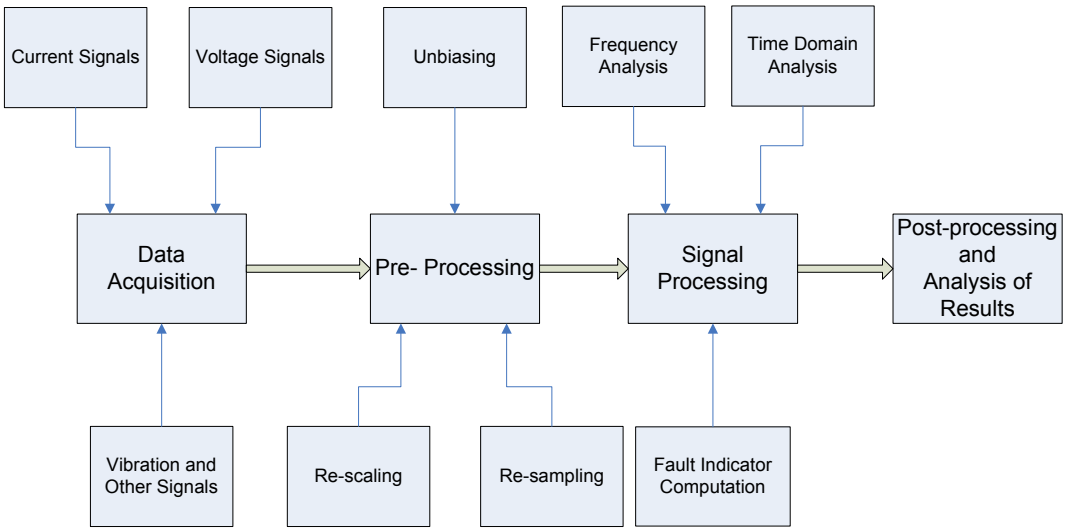

Fig. 4. Signal processing approach to fault diagnosis.

For example, frequencies associated with a broken rotor bar are given by the following formula,

$$f_{brb} = f_e \left[k\frac{(1-s)}{p/2} \pm s \right], \tag{3.1}$$

where, f_e is the electrical supply frequency k = 1,2,3,..., s is the per unit slip, p is the number of poles and due to the normal winding configuration, $2k/p$ =

$1, 5, 7, 11, 13, \ldots$.

The frequencies associated with a bearing fault are typically expressed as following,

$$f_{brng} = f_e \pm m \cdot f_\nu, \tag{3.2}$$

where $m = 1, 2, 3, \ldots$, and f_ν is one of the characteristic vibration frequencies. The characteristic vibration frequencies for ball bearings are computed using the bearing dimensions.

Evidently, the identification of these frequencies of interest requires, an intimate knowledge of the motor being monitored. The ability of a mechanical fault to manifest itself in some form in motor current frequency spectrum, thus, forms the basis for a robust mechanical fault detection system. The desired fault indicator, should be capable of quantifying the distortion in currents due to fault specific frequencies.

As, the vibration signals are directly affected by the mechanical condition of a motor, through its structure, they can be readily used for health assessment. Whereas electrical signals, inherently, are affected by the source that drives the motor and need more pre-processing than vibration signals. This work uses only electrical signals to make inferences about the machine health.

B. Processing of Electrical Signals

The electrical measurements from an induction motor are not readily presentable as means for health assessment. This section describes the procedure followed to obtain the fault indicators from raw electrical measurements. The processing described under this section is coded in MATLAB and is depicted as a flow-chart in Figure 5.

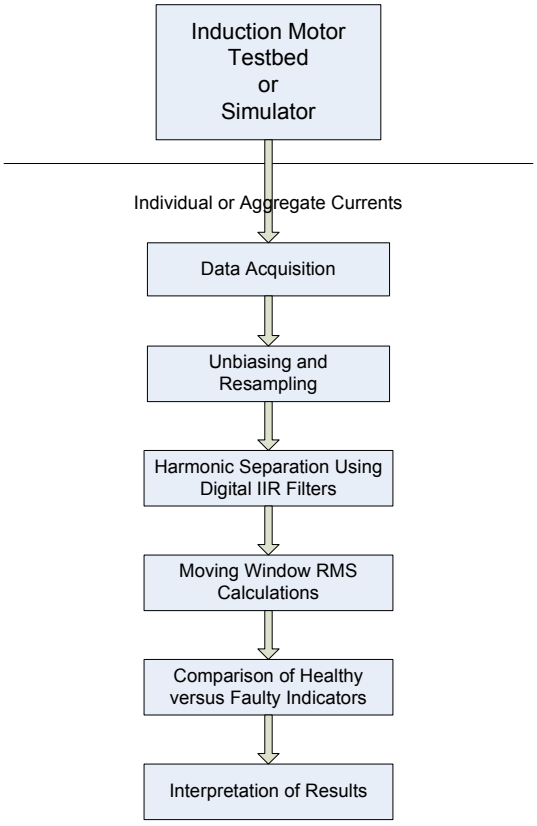

Fig. 5. Processing of electrical signals–flow chart.

1. Downsampling and Unbiasing

All signals are downsampled to a sampling rate at which the rest of the processing is done. Experimental data is sometimes associated with bias in some channels of the data acquisition system. The bias, if any, is removed by forcing the sinusoidal signals to a zero mean.

2. Harmonic Separation Using Digital Filters

The mechanical faults encountered in induction motors are known to affect only certain characteristic frequencies and/or associated with a rise in the noise floor of the current spectrum. The magnitude of the affected frequencies are extremely small in comparison to the magnitude of the fundamental and the odd harmonics. The fundamental and its odd harmonics tend to mask, the change in the spectrum due to the faults. To accentuate these subtle changes in the spectrum and to make them considerable, when represented in terms of a fault indicator, it is desirable to remove the fundamental and its odd harmonics.

The odd harmonics including the fundamental are removed using Infinite Impulse Response (IIR) digital filters, obtained from *fdatool* utility of MATLAB. Depending upon the sampling rate of the signal, F_s, odd harmonics up to $F_s/2$ are notched. Thus, the signals obtained after harmonic separation consisted of the even harmonics and the inter-harmonics.

Due to the steep attenuations of the notch filters that are used for harmonic separation, the resultant signal is found to have distortion. The distorted region of the processed signal is not considered for further processing.

3. Moving Average Root Mean Square Algorithm

The Root Mean Square (RMS) gives an average measure of the data under consideration. A moving window RMS on the other hand gives a measure of variation of the average values of the data over time.

The moving window RMS value of a signal $x(t)$, $t_1 \leq t \leq t_N$, is defined as follows:

$$x_{RMS}(l) = \sqrt{\int_{t_1+lp}^{t_2+lp} x(t)^2 dt}, \quad l = 0, 1, \ldots, m, \tag{3.3}$$

where $t_2 - t_1$ is the size of the moving window, with a moving window distance of p and $m = (t_N - t_2)/p$.

The length of the moving window used is the number of samples equivalent to five cycles of fundamental component of the current signal. The windowed RMS is calculated at every sample of the signal i.e., the window is moved by one sample throughout the length of the signal.

4. Current-Based Mechanical Fault Indicator

The moving window RMS signal of the processed currents, thus obtained, is indicative of the health of the motor. An average of the moving window RMS signal of each phase is calculated to obtain a single value per phase. The average of the three values corresponding to three phase currents, is termed as the fault indicator for the motor. Thus, a single value is obtained to indicate the health of the motor. This value henceforth will be termed, merely, as an "indicator". If $i^a_{RMS}(l)$, $i^b_{RMS}(l)$, $i^c_{RMS}(l)$ are the moving window RMS signals of the processed three phase currents. Furthermore, the following averaging is performed:

$$
\begin{aligned}
I_a &= \frac{1}{N}\sum_{l=1}^{N} i^a_{RMS}(l), \\
I_b &= \frac{1}{N}\sum_{l=1}^{N} i^b_{RMS}(l), \\
I_c &= \frac{1}{N}\sum_{l=1}^{N} i^c_{RMS}(l), and, \\
I &= \frac{1}{3}\left[I_a + I_b + I_c\right]
\end{aligned} \tag{3.4}
$$

where, N is the length of the RMS signal, I_a, I_b and I_c are the indicators for the three phases and I is the average fault indicator for the motor.

The indicator is calculated for both healthy and faulty cases. The presence of fault is determined by percentage relative change in the indicator from the healthy case. The healthy indicator increases with motor load increase. The indicator hence is always compared with the healthy indicator at the same motor load level.

C. Effectiveness of the Indicator Developed to Broken Rotor Bar Faults

The effectiveness of the indicator is first tested by applying the procedure described in the previous section to the currents obtained from a 800 hp Allis Chamber motor. The data is obtained at two different load levels and at different severities of broken rotor bar fault. The processing is done at a sampling rate of 960 samples per second after resampling it from 40,000 samples per second. Figure 6 depicts the variation of the indicator with load level and fault severity. Alongside, for every fault severity, the percentage variation of the corresponding indicator value from the healthy case is plotted. Note the changes in indicator values with load and fault severities. The horizontal line corresponding to 5% relative change in fault indicator represents the allowed variation under normal operating conditions. Such low fault indicator

changes, though indicative of faults of low severities, may also be caused due to small changes in load or changes in voltage source condition.

D. Chapter Summary

In this chapter, a motor–current based mechanical fault indicator is developed. The sequential procedure involved in computing the fault indicator from raw current measurements of a motor, is described.

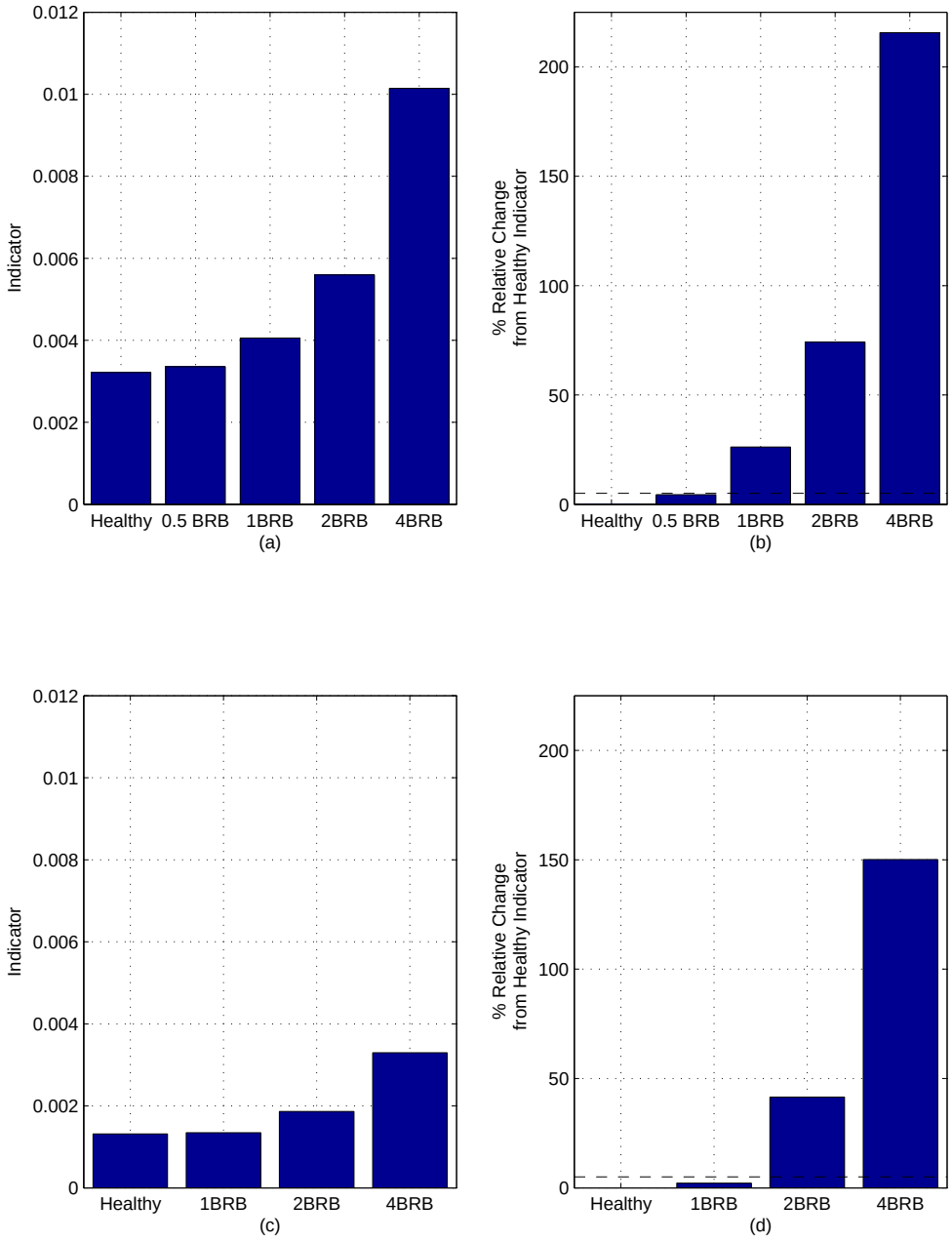

Fig. 6. Indicator value and percentage relative change from the healthy case, for 800 hp AC motor at different fault severities of broken rotor bars (BRB) and load levels; (a)&(b) 100% load; (c)&(d) 50% load.

CHAPTER IV

SIMULATED INVESTIGATION OF FAULT INDICATOR CHANGE IN MOTORS ENERGIZED BY A COMMON VOLTAGE BUS

A. Simulator

1. Description of the Simulations Performed

The Simulator is configured to simulate two detailed parameter models, viz., a 3–phase, 4 pole, 1 hp motor and a 3–phase, 4 pole, 7.5 hp motor. The latter is rated for 460V input, while the former is rated at 230V and 460V. Multiple motors of approximately same power rating are simulated by varying the resistance and inductance parameters of the original motor within ±5% of the original values. Thus no two simulated motors are identical. Twenty motors each of the three ratings are simulated for use in different analyses. The simulations are performed at three load levels and at different broken rotor bar fault severities. The load levels in increasing order of the load are designated as 'A', 'B' and 'C'. Table I shows the load levels and fault severities simulated for different motor ratings.

Table I. Load Levels and Fault Severities Simulated with the Available Motor Ratings

Motor Rating	Load Designation			Maximum Simulated Broken Rotor Bar Fault Severity
	A	B	C	
1 hp 230V	60%	80%	100%	5
1 hp 460V	80%	90%	100%	5
7.5hp 460V	50%	60%	70%	3

The inputs and outputs are obtained at a sampling rate of 1000 samples per second. The data is resampled to 960 samples per second and the measurements from the steady-state region of the motor operation are used for further processing.

2. Indicator Calculation for Single Motor

The procedure described in the section B of Chapter II, for obtaining indicators, is applied alike to the data obtained from experiments and simulations. Figures 7, 8 and 9, show the indicator and the percentage relative variation of faulty cases from the healthy case, for 1 hp 230V motor, 1 hp 460V motor and 7.5 hp 460V motor respectively.

3. Indicator Calculation for a Motor Bank

The simulations of each motor of a configuration are carried out separately and the aggregate currents are obtained as a sum of corresponding phase currents of the individual motors. The three phase aggregate currents, thus obtained, are processed according to the procedure described in section B of Chapter III, for fault indicators.

B. Degrees of Freedom in a Motor Bank

The analysis of using aggregate currents for detecting faults in motor banks can be carried out in different ways. Table II lists the degrees of freedom for such an analysis. It can be seen that the problem at hand in its unconstrained form is complicated.

1. Constraints Imposed by Simulations Performed

From the available ratings, shown in Table I , there are two ways of choosing motor ratings for a motor bank. One, an arrangement wherein all the motors are of same

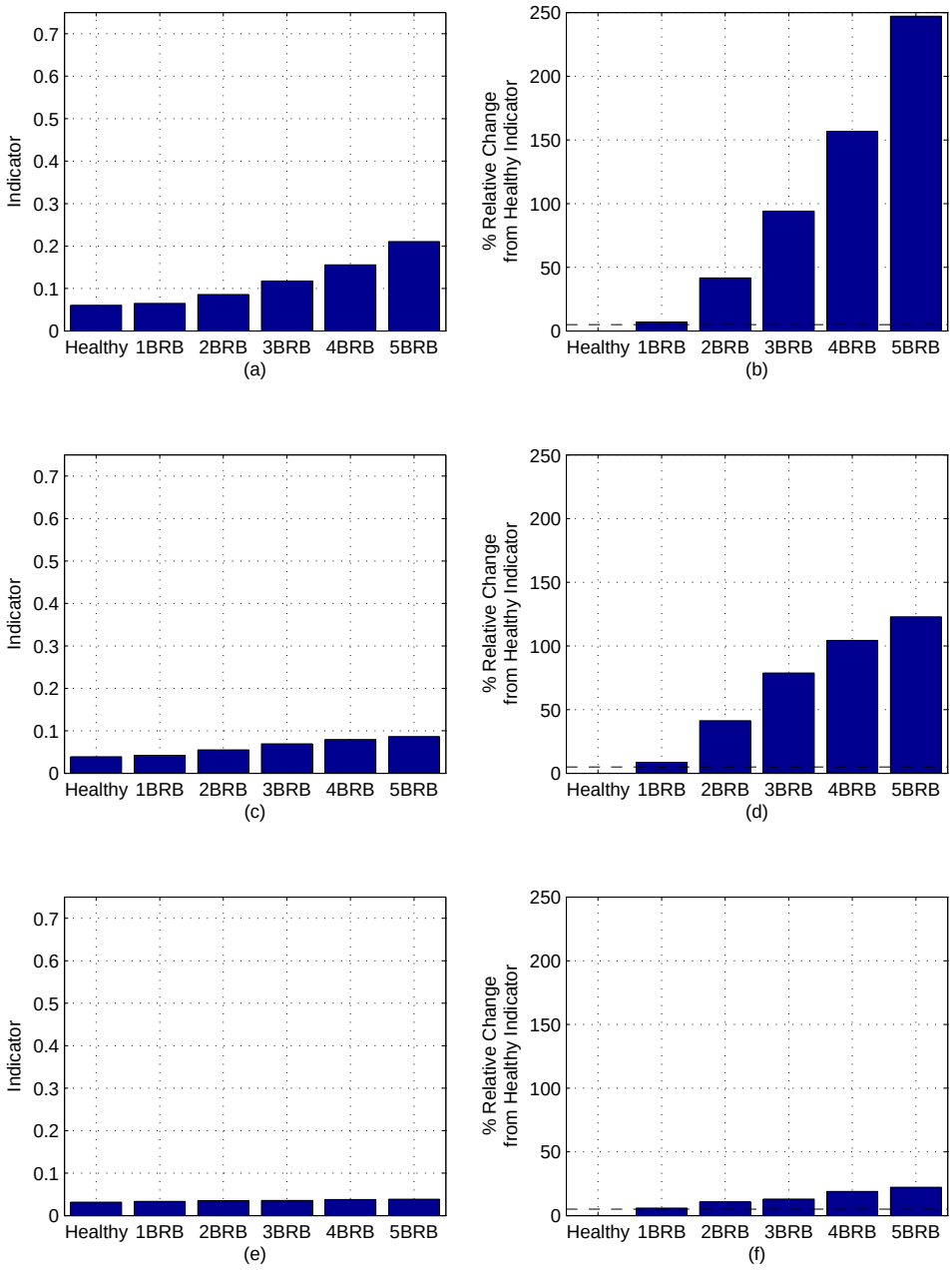

Fig. 7. Indicator value and percentage relative change from the healthy case, for 1 hp 230V motor at different fault severities of broken rotor bars (BRB) and load levels; (a)&(b) 100% load; (c)&(d) 80% load; (e)&(f) 60% load.

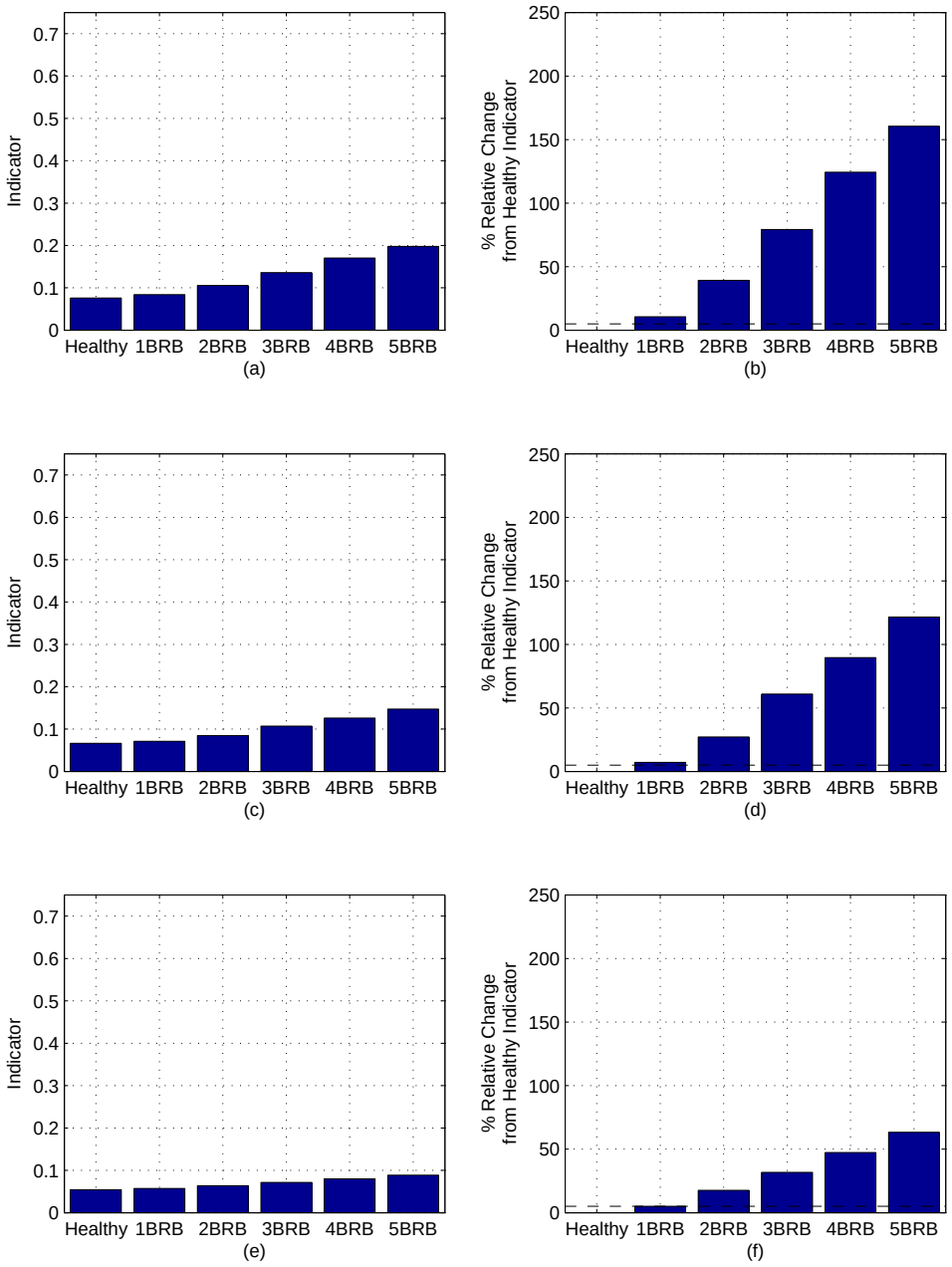

Fig. 8. Indicator value and percentage relative change from the healthy case for, 1 hp 460V motor at different fault severities of broken rotor bars (BRB) and load levels; (a)&(b) 100% load; (c)&(d) 90% load; (e)&(f) 80% load.

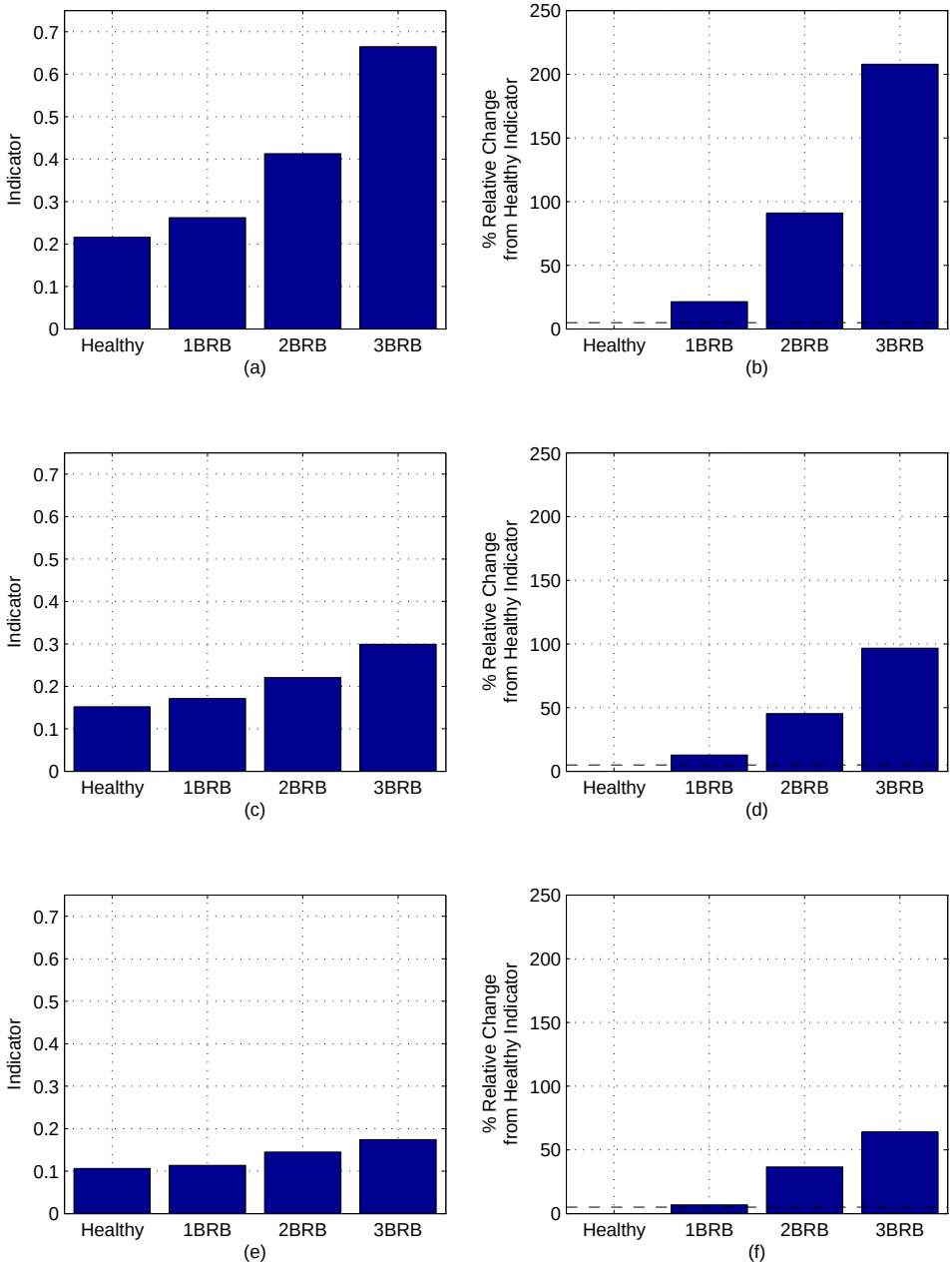

Fig. 9. Indicator value and percentage relative change from the healthy case, for 7.5 hp 460V motor at different fault severities of broken rotor bars (BRB) and load levels; (a)&(b) 70% load; (c)&(d) 60% load; (e)&(f) 50% load.

Table II. Degrees of Freedom for Aggregate Signature Analysis of Motor Banks

S.No.	Degree of Freedom
1	Number of motors
2	Motors rating
3	Motor load level
4	Number of faulty motors
5	Type of fault
6	Fault severity

rating and two, a combination of 1 hp and 7.5 hp motors. The choice of type of fault is constrained to be broken rotor bar. From the performed simulations, possible load levels on each motor of the motor bank are restricted to three.

2. Constraints Imposed by Assumptions

The problem is made more tractable by constraining load levels of the motor bank and fault severities in the faulty motors. Post-assumptions (section F of Chapter I), the degrees of freedom in a configuration (a motor bank with a specified number and power rating of motors) are reduced to load level of the healthy motors (l_h), load level of faulty motors (l_f), number of faulty motors (n) and fault severity of the faulty motors (fs). Symbolically, the configuration and the indicator obtained from its aggregate currents are denoted as $C_{[l_h,l_f],[n,fs]}$ and $I_{[l_h,l_f],[n,fs]}$, respectively.

3. Explanation for a Sample Configuration

Figure 10 shows a four motor configuration with two 1 hp and 7.5 hp motors, each. The two healthy motors, in accordance with the constraints imposed, are maintained

at same load level 'A', i.e., 1 hp motor at 80% load and 7.5 hp motor at 50% load. The two faulty motors are maintained at same load level 'C', i.e., 1 hp motor at 100% load and 7.5 hp motor at 70% load. Also, the fault severity in the faulty motors is three broken rotor bars, each. Thus, the specification for the configuration shown is $C_{[A,C],[2,3]}$. When the load level of the healthy motors is raised to 'C', the 1 hp motor is at 100% load and the 7.5 hp motor is at 70% load. The configuration specification, hence, is $C_{[C,C],[2,3]}$. If the fault severity of the configuration is increased to four broken rotor bars it implies that the faulty motors have a fault severity of four broken broken rotor bars, each. The configuration specification, in this case, is $C_{[C,C],[2,4]}$.

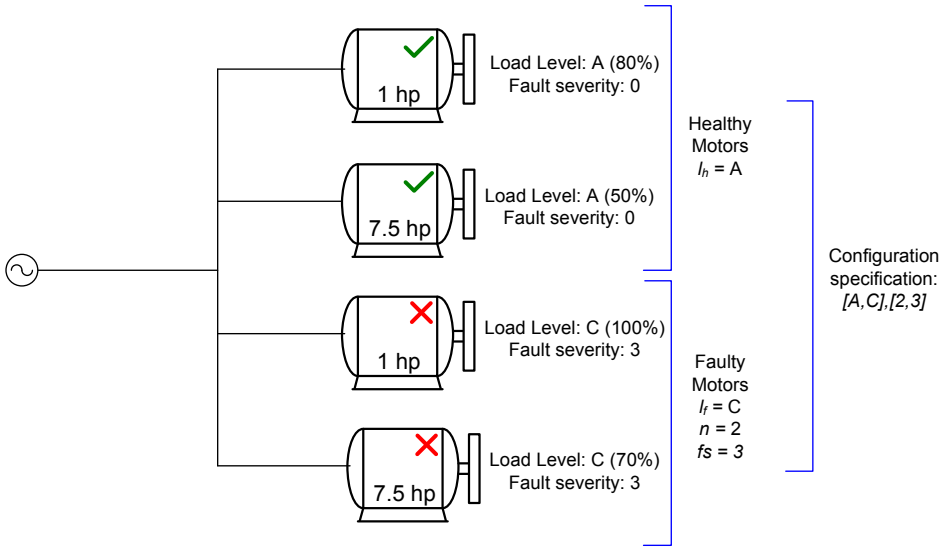

Fig. 10. A four-motor configuration; $C_{[A,C],[2,3]}$.

C. Definitions of Terms

The following quantities are defined for the presentation of the results in this chapter:

Healthy Rating, R_h : This is the sum of the rated power, in horse power (hp), of the healthy motors in a given configuration.

Faulty Rating, R_f : This is the sum of the rated power, in horse power (hp), of the faulty motors in a given configuration.

Total Rating, R_t : This is the sum of the rated power, in horse power (hp), of all the motors in a given configuration.

$$R_t = R_h + R_f \tag{4.1}$$

Healthy Motor Fraction, R_h/R_t : This is the ratio of healthy rating of a configuration to its total rating.

Faulty Motor Fraction, R_f/R_t : This is the ratio of faulty rating of a configuration to its total rating.

Fault Indicator Change (FIC), $FIC^C_{[l_h,l_f],[n,fs]}$: For a configuration C with m motors and n faulty motors, Fault Indicator Change is the percentage relative change in indicator from the healthy case at the same load level.

$$FIC^C_{[l_h,l_f],[n,fs]} = \frac{I^C_{[l_h,l_f],[n,fs]} - I^C_{[[l_h,l_f],[0,0]}}{I^C_{[l_h,l_f],[0,0]}} \times 100 \tag{4.2}$$

where $I^C_{[l_h,l_f],[0,0]}$ and $I^C_{[l_h,l_f],[n,fs]}$ are respectively the healthy and faulty indicator magnitudes for a configuration C;

FIC from a faulty motor's individual current measurements is ,

$$FIC^S_{[-,l_f],[1,fs]} = \frac{I^S_{[-,l_f],[1,fs]} - I^S_{[-,l_f],[0,0]}}{I^S_{[-,l_f],[0,0]}} \times 100 \tag{4.3}$$

An addition of healthy motors at load level l_h to the configuration S, would result in configuration HS and FIC from aggregate current measurements is expressed as,

$$FIC^{HS}_{[l_h,l_f],[1,fs]} = \frac{I^{HS}_{[l_h,l_f],[1,fs]} - I^{HS}_{[l_h,l_f],[0,0]}}{I^{HS}_{[l_h,l_f],[0,0]}} \times 100 \tag{4.4}$$

Fault Indicator Change Degradation, $D^{HS}_{[l_h,l_f],[1,fs]}$: This is the measure of reduction in FIC from aggregate measurements, as compared to FIC from faulty motor's individual measurements. It is defined mathematically as,

$$D^{HS}_{[l_h,l_f],[1,fs]} = \frac{FIC^{HS}_{[l_h,l_f],[1,fs]} - FIC^{S}_{[-,l_f],[1,fs]}}{FIC^{S}_{[-,l_f],[1,fs]}} \times 100 \tag{4.5}$$

where $FIC^{S}_{[-,l_f],[1,fs]}$ is the FIC of a single motor configuration S for a fault of fault severity fs and at load level l_f and $FIC^{HS}_{[l_h,l_f],[1,fs]}$ is the FIC for the configuration formed due to addition of healthy motors at load level l_h to the configuration S.

Henceforth, a single motor configuration would be termed as a 'reference' configuration, as it acts as the reference for study of degradation of FIC.

Figure 11 depicts a demonstration of the terms defined in this section for a four-motor configuration with a single faulty motor.

D. Problem Definition

The feasibility of using aggregate currents for detection of faults in motor banks can be investigated in several ways. Variation of two of the degrees of freedom, viz., number of motors in the motor bank and number of faulty motors in a given configuration

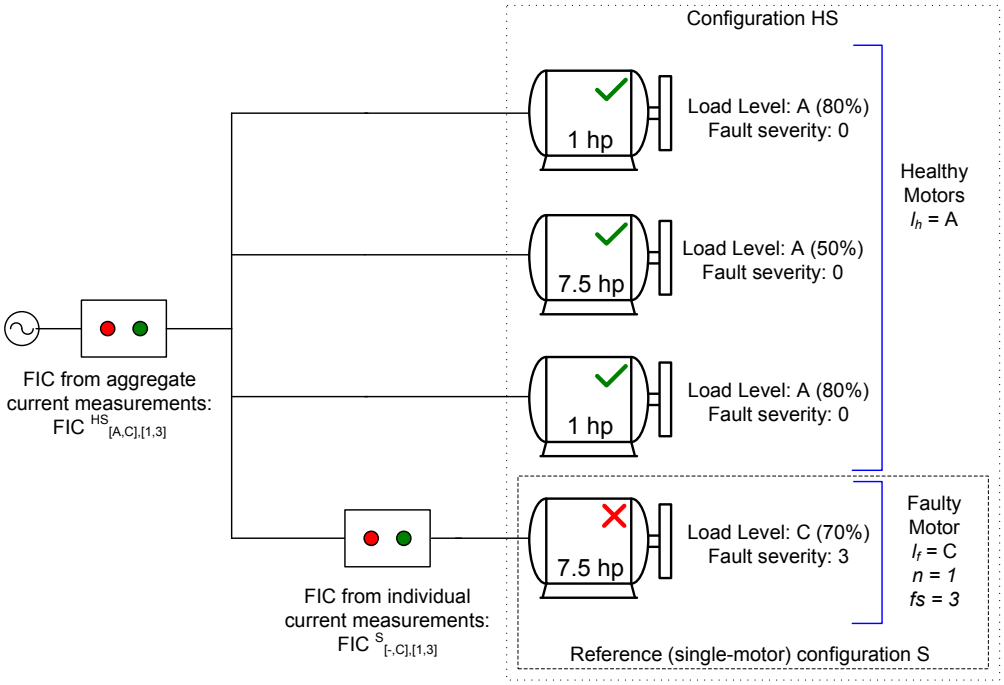

$$Degradation, D^{HS}{}_{[A,C],[1,3]} = \frac{FIC^{HS}{}_{[A,C],[1,3]} - FIC^{S}{}_{[-,C],[1,3]}}{FIC^{S}{}_{[-,C],[1,3]}} \times 100$$

$$HealthyMotorFraction, \frac{R_h}{R_t} = \frac{1+7.5+1}{1+7.5+1+7.5} = \frac{9.5}{17} = 0.56$$

$$FaultyMotorFraction, \frac{R_f}{R_t} = \frac{7.5}{1+7.5+1+7.5} = \frac{7.5}{17} = 0.44$$

Fig. 11. Fault Indicator Change, Degradation, Healthy Motor Fraction and Faulty Motor Fraction of a four-motor configuration.

are used here for the desired analysis. Accordingly, the simulation study is aimed at answering following questions:

1. Problem A - How does Fault Indicator Change (FIC), vary, when the same faulty motor is present in different healthy configurations?
2. Problem B - In a fixed configuration, how does the Fault Indicator Change (FIC), vary, as the number of faulty motors increase?

E. Simulation Results from Problem A

In Problem A, the aim is to study the variation in Fault Indicator Change (FIC) when a single faulty motor with broken rotor bar faults is present in different configurations.

Initially the analysis of faults in a 1 hp motor is presented, followed by the same for a 7.5 hp motor. Three cases each are presented for both the motors, for studying the effect of varying load levels on healthy and faulty motors of the configuration.

1. Explanation for a Sample Result Set

Table III shows the configurations with a faulty 1 hp 460V motor, employed to study the variation of FIC. It also shows the number of healthy and faulty motors. The load level on healthy and faulty motors of the configuration is 'A' and 'C', respectively. Note the presence of the faulty 1 hp motor in each configuration. The last column lists the corresponding Healthy Motor Fraction. Figure 12 depicts some of the configurations used.

The first configuration is the "reference" configuration with a single 1 hp motor. The subsequent configurations are obtained by adding corresponding healthy motors to the first configuration. Any variation in FIC with addition of healthy motors is compared with the FIC of the reference configuration (Degradation).

Table III. Configurations Used for Fault Indicator Change Analysis for a Faulty 1 hp Motor

S.No.	Number of Motors					Healthy Motor Fraction, R_h/R_t
	Healthy		Faulty		Total (Faulty)	
	1 hp	7.5 hp	1 hp	7.5 hp		
1	0	0	1	0	1 (1)	0.00
2	1	0	1	0	2 (1)	0.50
3	2	0	1	0	3 (1)	0.67
4	0	1	1	0	2 (1)	0.88
5	1	1	1	0	3 (1)	0.89
6	0	2	1	0	3 (1)	0.94
7	1	3	1	0	5 (1)	0.96
8	4	5	1	0	10 (1)	0.97

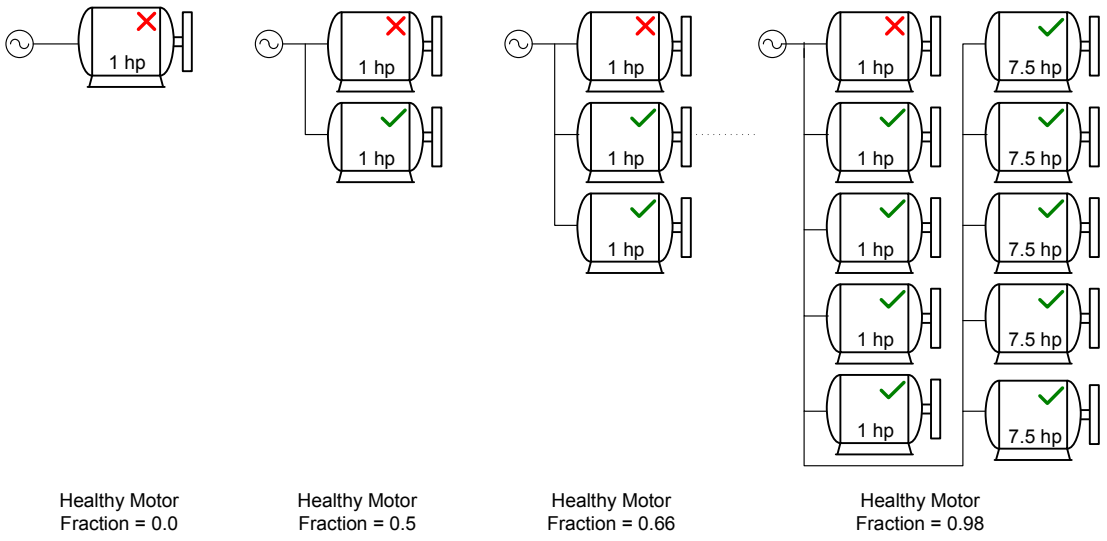

Fig. 12. A faulty 1 hp 460V motor in different configurations containing healthy 1 hp and 7.5 hp motors; configuration specification: $C^{1-8}_{[A,C],[1,3]}$.

Figure 13 shows FIC for different configurations in Table III, for a three broken rotor bar (BRB) fault in the 1 hp motor. A Healthy Motor Fraction of zero corresponds to the reference configuration and the FIC for this case is obtained by simulating 1 hp motor at 'C' (100%) load level both in faulty (3 BRB) and healthy conditions. FIC is calculated using Equation (4.3) and the value (80%) is plotted against a value of zero. A Healthy Motor Fraction of 0.5 is obtained by adding a healthy 1 hp motor, at load level 'A' (80%), to the existing one. The two motor configuration is simulated in healthy and faulty conditions (fault on the 1 hp motor at 'C' load level). The value (58%) obtained, using Equation (4.4), is plotted against a value of 0.5. Similarly, FIC for other configurations are obtained and plotted against their respective Healthy Motor Fraction values.

Figure 14 shows the Degradation of FIC for a three broken rotor bar fault in the 1 hp motor, with Healthy Motor Fraction, R_h/R_t, on x-axis. The Degradation

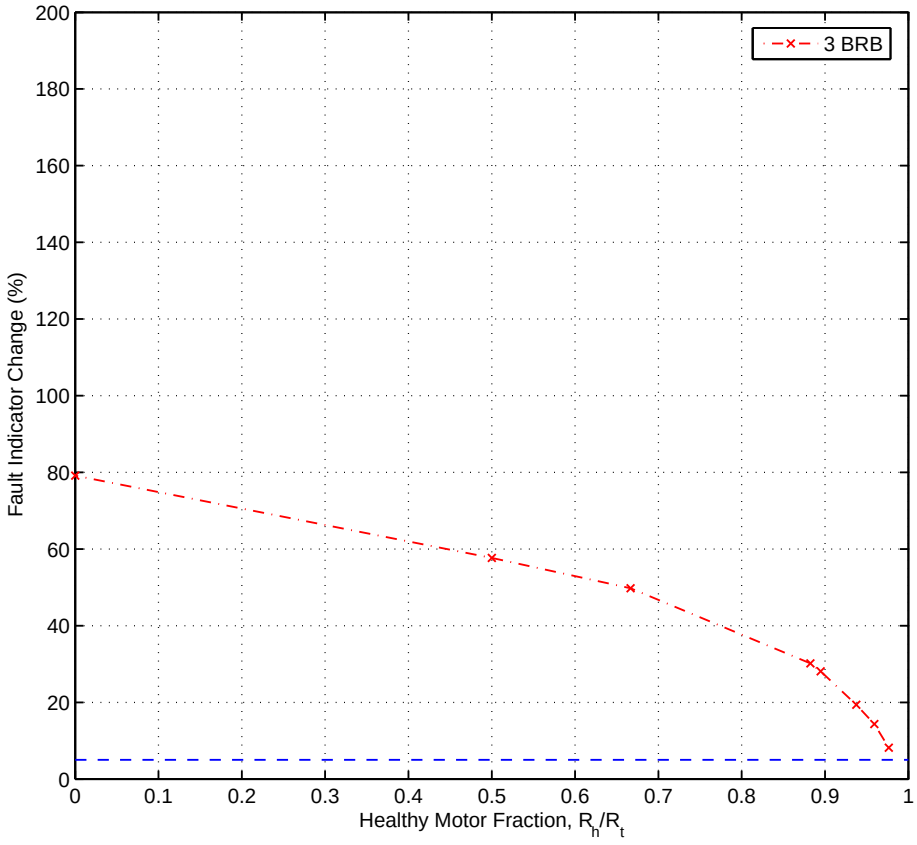

Fig. 13. Variation of Fault Indicator Change, when multiple healthy motors of 1 hp and 7.5 hp are placed in the same bank as a 1 hp 460V motor with three broken rotor bars (BRB) fault; configuration specification: $C^{1-8}_{[A,C],[1,3]}$.

values are obtained using Equation (4.5), by comparing FIC values of different configurations with that of the reference configuration. There cannot be any degradation for the stand-alone motor corresponding to a Healthy Motor Fraction of zero. For configuration two, with a Healthy Motor Fraction of 0.5, the reduction in FIC from that of the reference configuration, from the discussion above, is 22% and percentage relative change is about –27%. Similarly, degradations for other configurations are obtained and plotted against their respective Healthy Motor Fraction values. Note the negative sign on the y-axis, corresponding to the degradation.

Symbolically, the above discussion,

$$\begin{aligned}
FIC^1_{[-,C],[1,3]} &= 80\%, \\
FIC^2_{[A,C],[1,3]} &= 58\%, \\
D^1_{[-,C],[1,3]} &= \frac{FIC^1_{[-,C],[1,3]} - FIC^1_{[-,C],[1,3]}}{FIC^1_{[-,C],[1,3]}} \times 100 \\
&= \frac{(80-80)}{80} \times 100 \\
&= 0\% \\
D^2_{[A,C],[1,3]} &= \frac{FIC^2_{[A,C],[1,3]} - FIC^1_{[-,C],[1,3]}}{S^1_{[-,C],[1,3]}} \times 100 \\
&= \frac{(58-80)}{80} \times 100 \\
&= -27\%
\end{aligned} \tag{4.6}$$

where the superscripts $1, 2, \ldots$, represent configuration numbers listed in Table III, A and C are the load levels on healthy and faulty motors of the configurations and 3 in subscript is the fault severity.

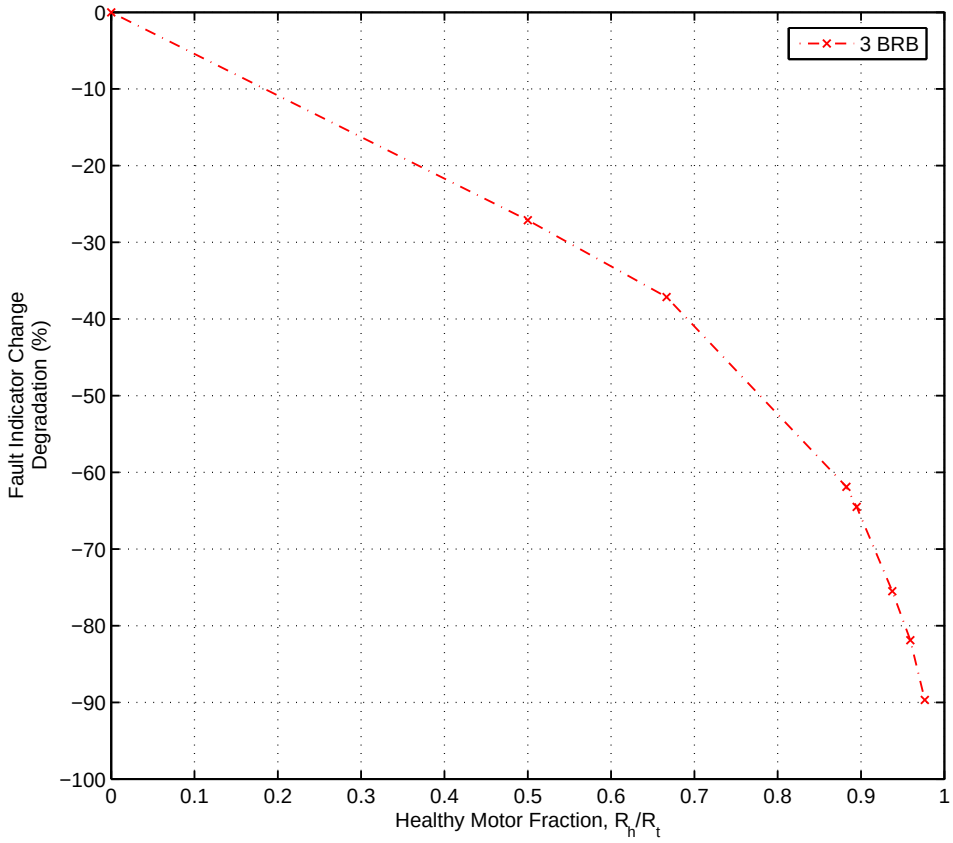

Fig. 14. Variation of Fault Indicator Change Degradation, when multiple healthy motors of 1 hp and 7.5 hp are placed in the same bank as a 1 hp 460V motor with three broken rotor bars (BRB) fault; configuration specification: $C^{1-8}_{[A,C],[1,3]}$.

2. Fault Indicator Change Analysis of a 1 hp Faulty Motor

Table III shows the configurations used for the studying the variation of FIC for a faulty 1 hp motor. Thus the 1 hp motor is the reference configuration. FIC variation is studied for different fault severities of up to five broken rotor bars in the 1 hp motor.

Figure 15 shows FIC variation among the configurations of Table III with different fault severities in the faulty 1 hp motor. The load levels on healthy and faulty motors is 'A' and 'C' respectively, corresponding to Case I of Table IV. As expected the faults of all severities are best detected when the faulty motor is stand-alone, corresponding to a Healthy Motor Fraction of zero. As more motors, in terms of horse power, are added to the 1 hp motor, corresponding to increasing values of Healthy Motor Fraction, FIC drops across all the fault severities, due to increase in the value of the healthy indicator. Also, as the Healthy Motor Fraction gets closer to the value of 1.0, the distinction between FIC for different fault severities gets difficult.

Figure 16 shows the degradation in FIC for configurations of Table III with different fault severities in the 1 hp motor. Degradation for different fault severities are calculated using the corresponding FIC of the reference configuration. As the number of healthy motors increase, the degradation in FIC increases up to 90%. An interesting observation of the degradation plot is that FIC for different fault severities degrade by approximately same amount for each configuration.

a. Effect of Load of the Configuration

The FIC in case of a broken rotor bar fault, increases with increase in the load on the motor. While an increase in load level of a single faulty motor enables easier detection of fault in it, the consequence of variation in load levels on healthy and faulty motors

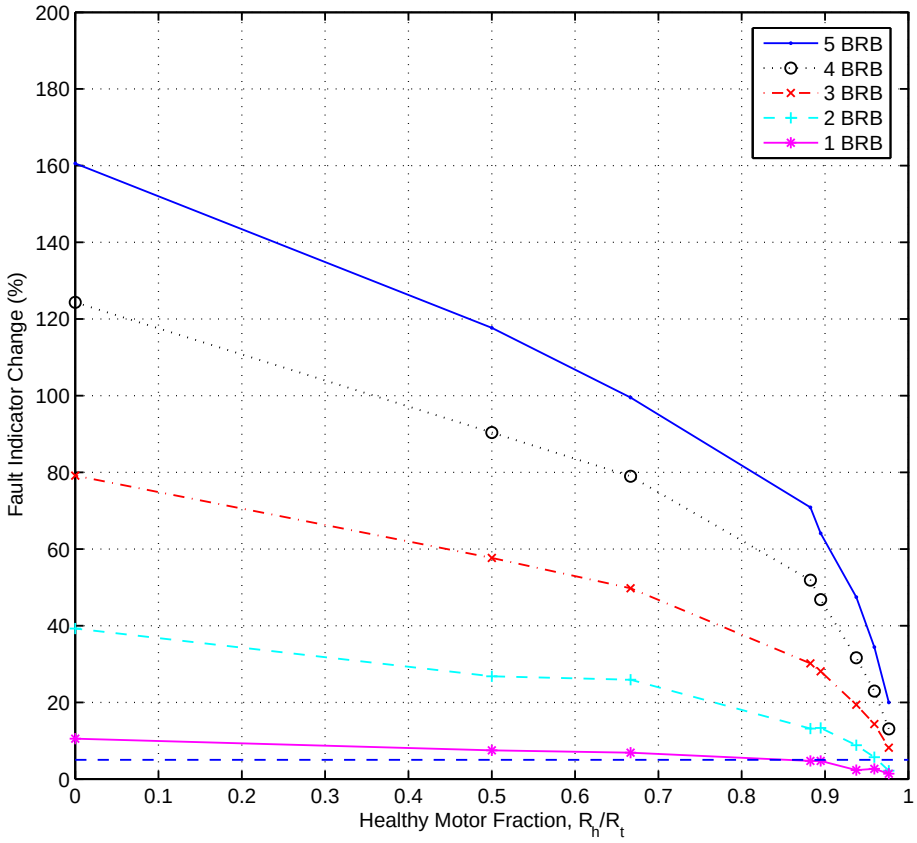

Fig. 15. Variation of Fault Indicator Change, when multiple healthy motors of 1 hp and 7.5 hp are placed in the same bank as a 1 hp 460V motor with broken rotor bar (BRB) faults; configuration specification: $C^{1-8}_{[A,C],[1,1-5]}$.

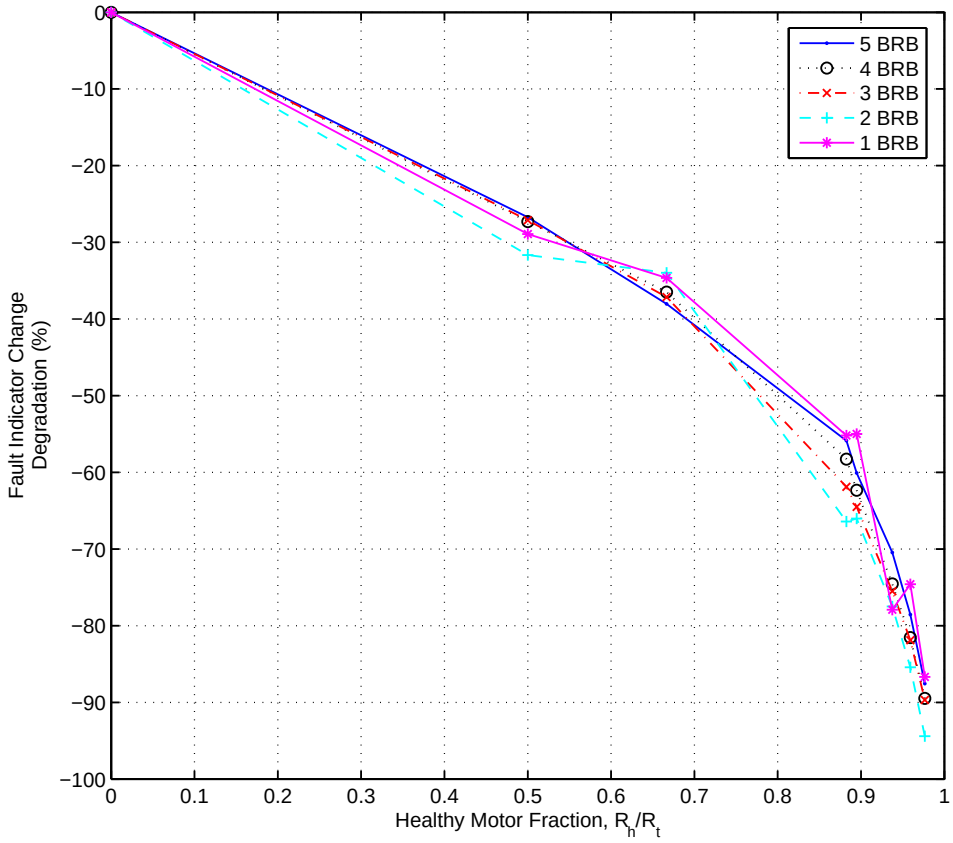

Fig. 16. Variation of Fault Indicator Change Degradation, when multiple healthy motors of 1 hp and 7.5 hp are placed in the same bank as a 1 hp 460V motor with broken rotor bar (BRB) faults; configuration specification: $C^{1-8}_{[A,C],[1,1-5]}$.

Table IV. Different Cases of Load Levels of Configurations in Table III, Used for Studying Effect of Load Level on Fault Indicator Change Variation; 1 hp Motor Faulty.

Case	Load Level of	
	Healthy Motors	Faulty Motors
I	A	C
II	C	C
III	C	A

of a configuration is of interest. Towards this end, three different load levels of healthy and faulty motors are simulated as listed in Table IV. The three cases represent the two extreme load levels and an intermediate load level of the configurations. Figure 17 shows the FIC variation for the same. The fault severity in the 1 hp motor is three broken rotor bars. Figure 18 shows corresponding FIC degradation.

Though the trend of drop in FIC with increase in Healthy Motor Fraction persists in all the three cases, it is evident that in Case–I, the degradation is "slower" than the other two cases. That means, for a given configuration, a lesser drop in FIC with increasing Healthy Motor Fraction than the other two cases. The other extreme being Case–III. While higher load level on the faulty motor is desirable, lower load levels on healthy motors is conducive for broken rotor bar fault detection from aggregate current measurements.

3. Fault Indicator Change Analysis of a 7.5 hp Faulty Motor

Table V shows the configurations used for studying the variation of FIC for faults in a 7.5 hp motor. The first configuration, i.e., the stand alone 7.5 hp motor, is the

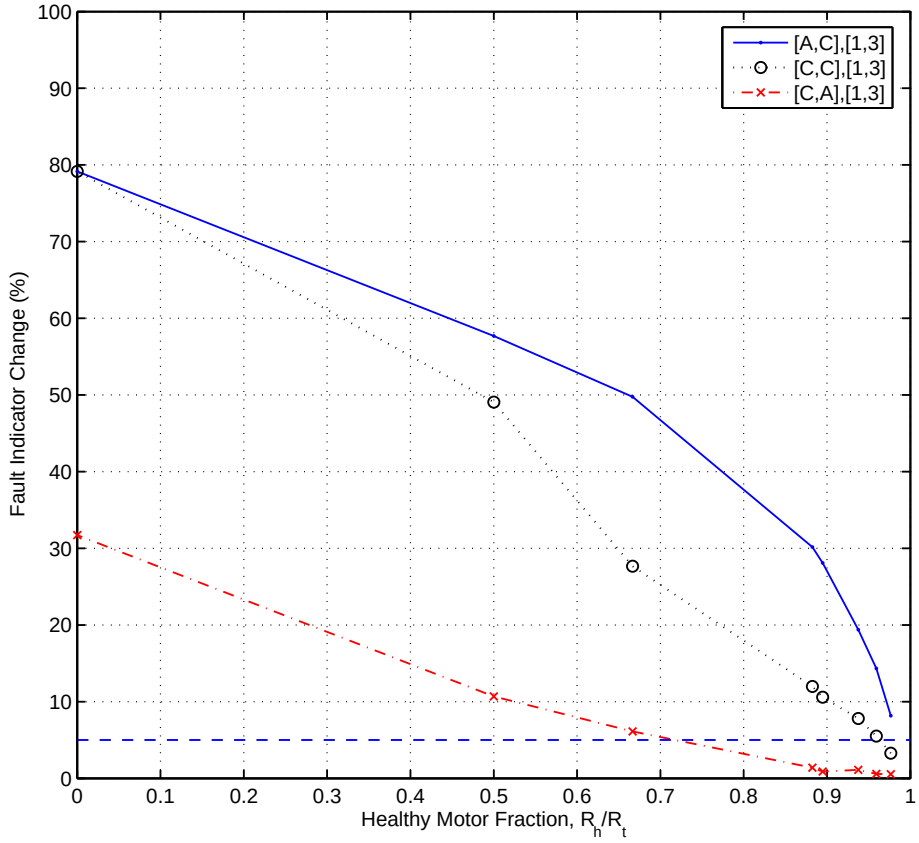

Fig. 17. Effect of load level of the configuration; variation of Fault Indicator Change, when multiple healthy motors of 1 hp and 7.5 hp are placed in the same bank as a 1 hp 460V motor with three broken rotor bars (BRB) fault.

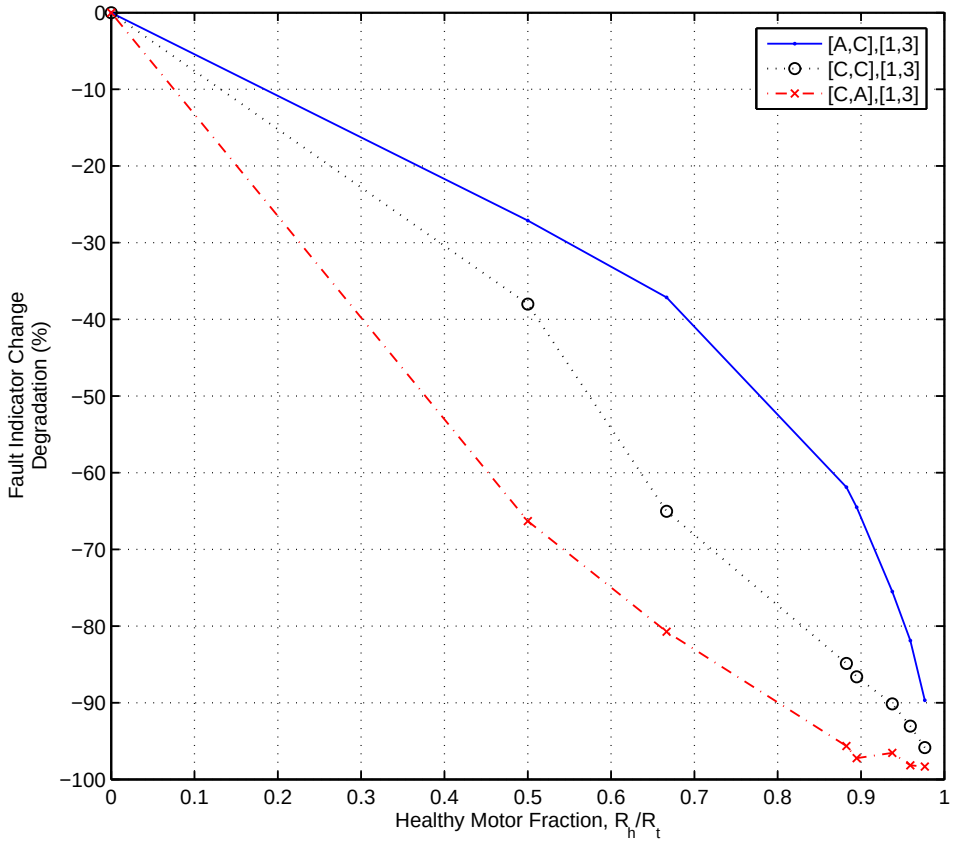

Fig. 18. Effect of load level of the configuration; variation of Fault Indicator Change Degradation, when multiple healthy motors of 1 hp and 7.5 hp are placed in the same bank as a 1 hp 460V motor with three broken rotor bars (BRB) fault.

Table V. Configurations Used for Fault Indicator Change Analysis for a Faulty 7.5 hp Motor

S.No.	Number of Motors					Healthy Motor Fraction, R_h/R_t
	Healthy		Faulty		Total (Faulty)	
	1 hp	7.5 hp	1 hp	7.5 hp		
1	0	0	0	1	1 (1)	0.00
2	1	0	0	1	2 (1)	0.12
3	2	0	0	1	3 (1)	0.21
4	0	1	0	1	2 (1)	0.50
5	1	1	0	1	3 (1)	0.53
6	0	2	0	1	3 (1)	0.67
7	2	2	0	1	5 (1)	0.70
8	5	4	0	1	10 (1)	0.82

reference configuration. Variation is studied for fault severities of up to three broken rotor bars.

Figure 19 shows FIC variation among the configurations of Table V with different fault severities in 7.5 hp motor. The load levels on healthy and faulty motors is 'A' and 'C' respectively. The variation in FIC with addition of healthy motors to 7.5 hp motor is marginal, initially, but is considerable as the Healthy Motor Fraction becomes closer to one. Also, in this case, the distinction between FIC for different fault severities exists even at higher Healthy Motor Fractions.

Figure 20 shows the degradation in FIC for configurations of Table V with different fault severities on the faulty 7.5 hp motor. As Healthy Motor Fraction increases, the degradation increases to about 50% at higher values. Even in this case, as in

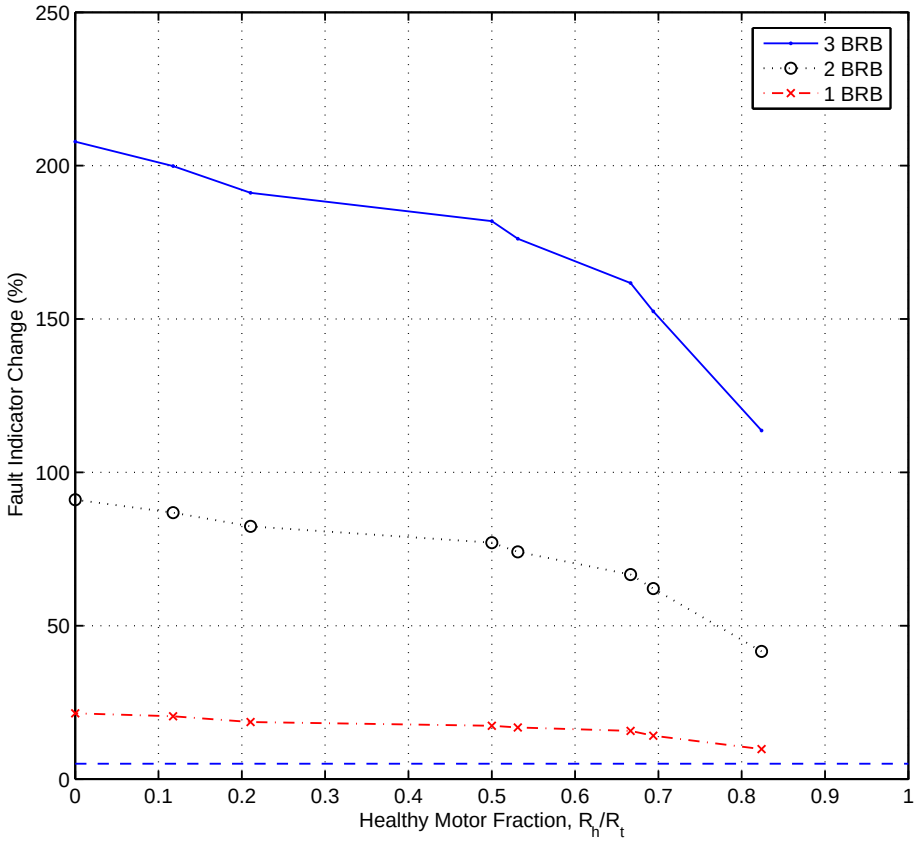

Fig. 19. Variation of Fault Indicator Change, when multiple healthy motors of 1 hp and 7.5 hp are placed in the same bank as a 7.5 hp 460V motor with broken rotor bar (BRB) faults; configuration specification: $C^{1-8}_{[A,C],[1,1-3]}$.

the case of 1 hp motor, FIC for different fault severities degrades by approximately same amount for each configuration. Lesser degradation for similar load conditions and configurations, in case of 7.5 hp motor when compared to 1 hp motor, can be explained through the higher contribution of a 7.5 hp motor with a broken rotor bar fault towards indicator than that of a 1hp motor with the same fault.

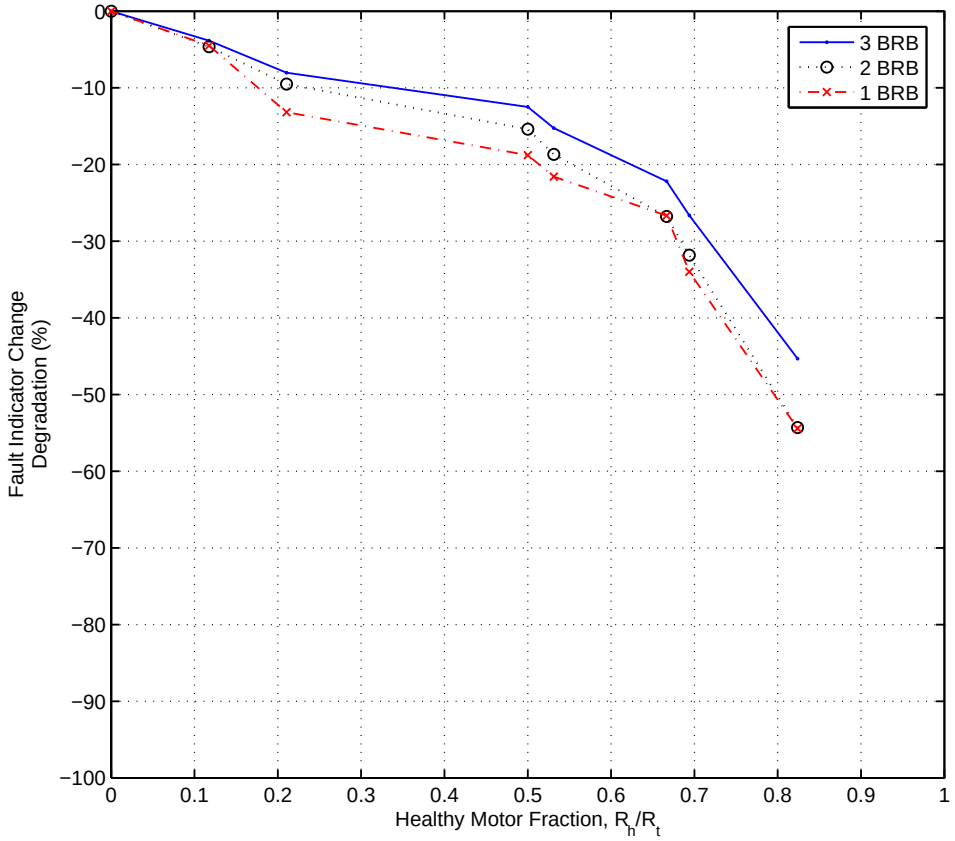

Fig. 20. Variation of Fault Indicator Change Degradation, when multiple healthy motors of 1 hp and 7.5 hp are placed in the same bank as a 7.5 hp 460V motor with broken rotor bar (BRB) faults; configuration specification: $C^{1-8}_{[A,C],[1,1-3]}$.

Table VI. Different Cases of Load Levels of Configurations in Table V, Used for Studying Effect of Load Level on Fault Indicator Change Variation; 7.5 hp Motor Faulty.

Case	Load Level of	
	Healthy Motors	Faulty Motors
I	A	C
II	C	C
III	C	A

a. Effect of Load of the Configuration

Three cases of different load levels on healthy and faulty motors of the configurations are simulated as listed in Table VI. Figure 21 shows the FIC variation for the same. The fault severity in the 7.5 hp motor is two broken rotor bars. Figure 22 shows the corresponding FIC degradation.

The drop in FIC is more pronounced in the Case–III than compared to the rest of the cases. It can be seen that, the degradation curve changes shape from convex to concave from Case–I to Case–III. Following the trend, one could expect that for a case with higher load on the faulty 7.5 hp motor and lower load on the healthy motors, than what is listed under Case–I, the degradation curve to be more convex.

F. Simulation Results from Problem B

This approach is followed to study the variation of Fault Indicator Change (FIC) in a fixed configuration with increasing number of faulty motors. The number of motors in the configuration is twenty and ten motors are made faulty, starting with one faulty motor and ending with ten. As the number of faulty motors is increased, the variation

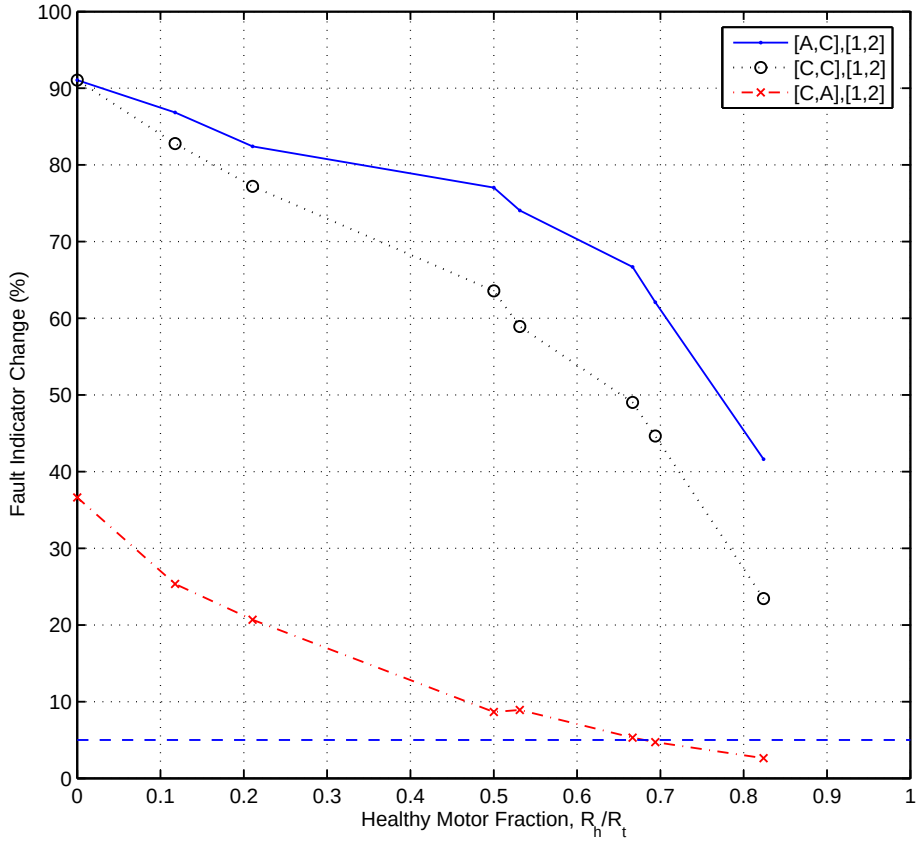

Fig. 21. Effect of load level of the configuration; Variation of Fault Indicator Change, when multiple healthy motors of 1 hp and 7.5 hp are placed in the same bank as a 7.5 hp 460V motor with two broken rotor bar (BRB) fault.

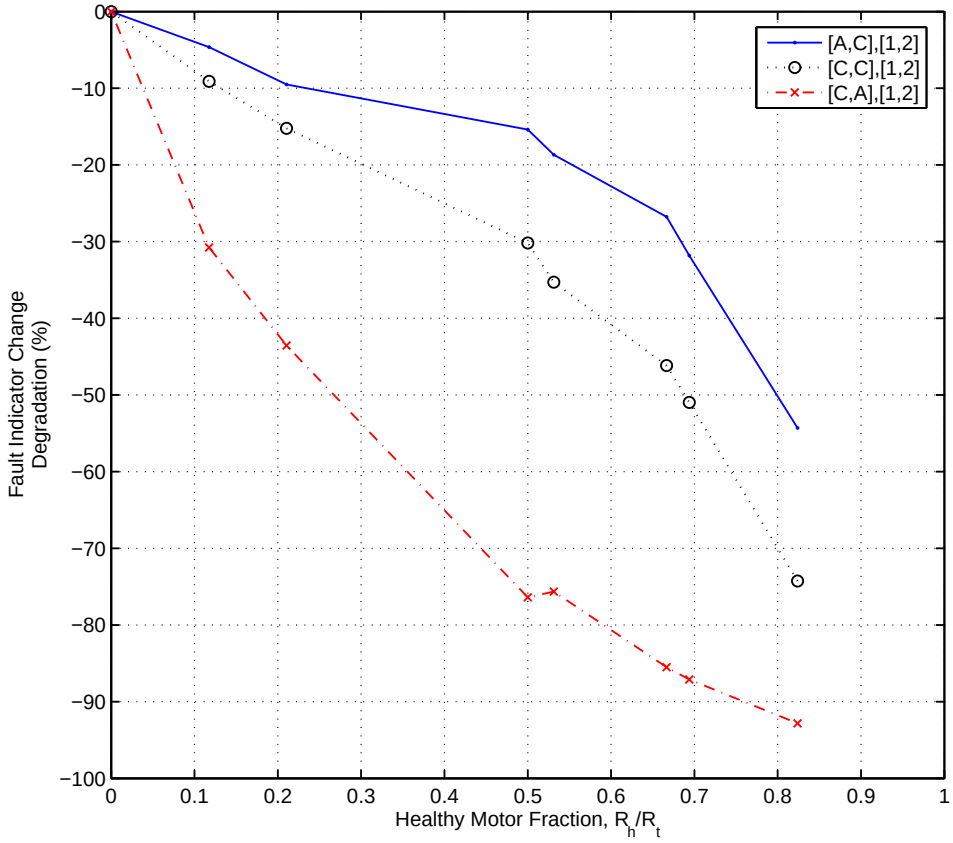

Fig. 22. Effect of load level of the configuration; Variation of Fault Indicator Change Degradation, when multiple healthy motors of 1 hp and 7.5 hp are placed in the same bank as a 7.5 hp 460V motor with two broken rotor bar (BRB) fault.

Table VII. Faulty Ratios for Increasing Number of Faulty Motors in a 20 Motor Configuration

S. No.	Number of Motors			Faulty Motor Fraction, R_f/R_t
	Healthy	Faulty	Total	
1	20	0	20	0.00
2	19	1	20	0.05
3	18	2	20	0.10
4	17	3	20	0.15
5	16	4	20	0.20
6	15	5	20	0.25
7	14	6	20	0.30
8	13	7	20	0.35
9	12	8	20	0.40
10	11	9	20	0.45
11	10	10	20	0.50

of FIC can be studied with respect to the Faulty Motor Fraction (R_f/R_t). Table VII shows the different Faulty Ratios corresponding to increasing number of faulty motors. The configurations consisted of motors of same power rating, to discount the difference in contributions of faulty motors of different power rating, towards the indicator. Two configurations as listed in Table VIII are used for investigating this problem. Initially, results from the configuration containing 1 hp 230V motors are presented, followed by the same for 7.5 hp 460V motors. In both the cases the load level on healthy and faulty motors of the configuration is 'C'.

Table VIII. Configurations Used in Problem B

Configuration			Load Level	
No.	Motor Rating	Number of Motors	Healthy	Faulty
1	1 hp 230V	20	C	C
2	7.5 hp 460V	20	C	C

The variation of FIC is also studied at different fault severities of the faulty motors of the configuration. For the first configuration of Table VIII, fault severities of up to five broken rotor are simulated and for the second configuration fault severities of up to three broken rotor bars are simulated.

1. Explanation for Sample Result Set

Figure 23 depicts a configuration of 20 motors, all 1 hp 230V, with different Faulty Motor Fractions. Figure 24 shows the variation of FIC for a five broken rotor bar fault, in the configuration with increasing number of faulty motors.

Table VII shows the Faulty Motor Fractions corresponding to different number of faulty motors. The first entry corresponds to the healthy configuration and the indicator value obtained for it is the healthy indicator, with which the indicator obtained for the rest of the entries is compared, to obtain respective FIC. First the simulation corresponding to first entry, i.e., all healthy, is performed and the healthy indicator value is 0.29. Next, the indicator corresponding to the second entry, i.e., one motor faulty with a five broken rotor bar fault with nineteen healthy motors, is calculated and the value is 0.37. Indicator corresponding to the third entry with, two out of twenty motors, faulty, is 0.46. FIC for the above two faulty cases are calculated using Equation 4.2 and are found to be approximately 27% and 57% respectively.

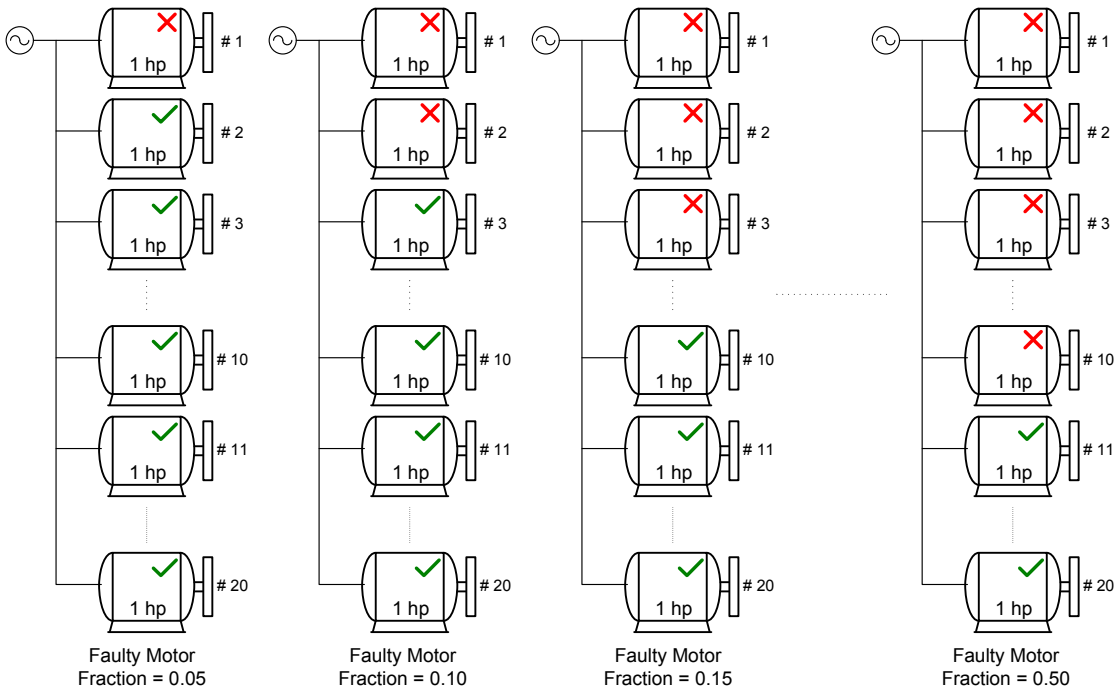

Fig. 23. 1 hp 230V motor configuration with increasing number of faulty motors; configuration specification: $C_{[C,C],[1-10,5]}$.

These values are plotted against their respective Faulty Motor Fraction values. The procedure is repeated for the remaining Faulty Motor Fraction values to obtain rest of the plot. The above discussion, symbolically, is shown under,

$$\begin{aligned}
I^1_{[C,C],[0,0]} &= 0.29 \\
I^1_{[C,C],[1,5]} &= 0.37 \\
I^1_{[C,C],[2,5]} &= 0.46 \\
FIC^1_{[C,C],[1,5]} &= \frac{I^1_{[C,C],[1,5]} - I^1_{[C,C],[0,0]}}{I^1_{[C,C],[0,0]}} \times 100 \\
&= \frac{0.37 - 0.29}{0.29} \times 100 \\
&= 27\% \\
FIC^1_{[C,C],[2,5]} &= \frac{I^1_{[C,C],[2,5]} - I^1_{[C,C],[0,0]}}{I^1_{[C,C],[0,0]}} \times 100 \\
&= \frac{0.46 - 0.29}{0.29} \times 100 \\
&= 57\%
\end{aligned} \tag{4.7}$$

where the super-script 1 indicates the configuration number from Table VIII.

2. Variation of Fault Indicator Change in a Fixed Configuration

a. 1 hp Motor Configuration

Figure 25 shows variation of FIC with increasing number of faulty motors in a configuration of twenty 1 hp 230V motors. The variation of FIC is studied with different fault severities on the faulty motors. Up to five broken rotor bars are simulated on the faulty motors, represented by different curves on the plot. It can be seen that in the case of higher fault severities, FIC increases with the number of faulty motors, but

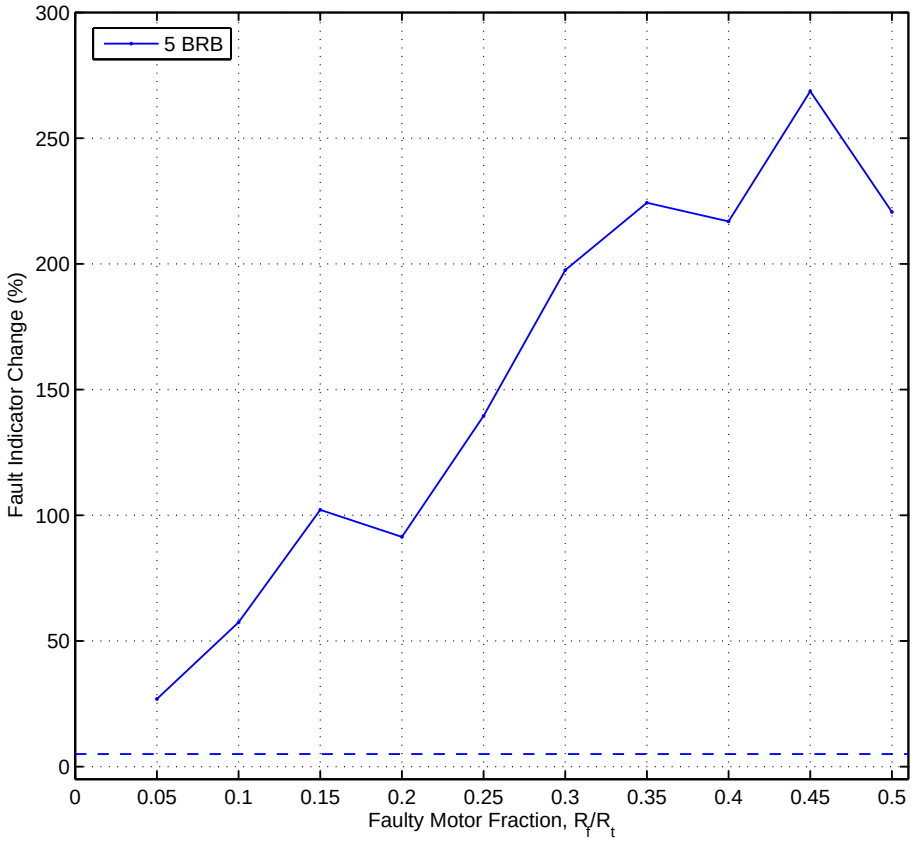

Fig. 24. Variation of Fault Indicator Change, in a configuration of twenty 1 hp 230V motors, with increasing number of faulty motors each having a five broken rotor bar fault; configuration specification: $C_{[C,C],[1-10,5]}$.

the increase is small for lower fault severities. This can be explained by, lower contribution of lower fault severities towards the fault indicator and also by the presence of healthy motors at load level 'C' in addition to the faulty motors. The 'oscillatory' nature of the curves can be explained by the difference in motor parameters of the individual faulty motors.

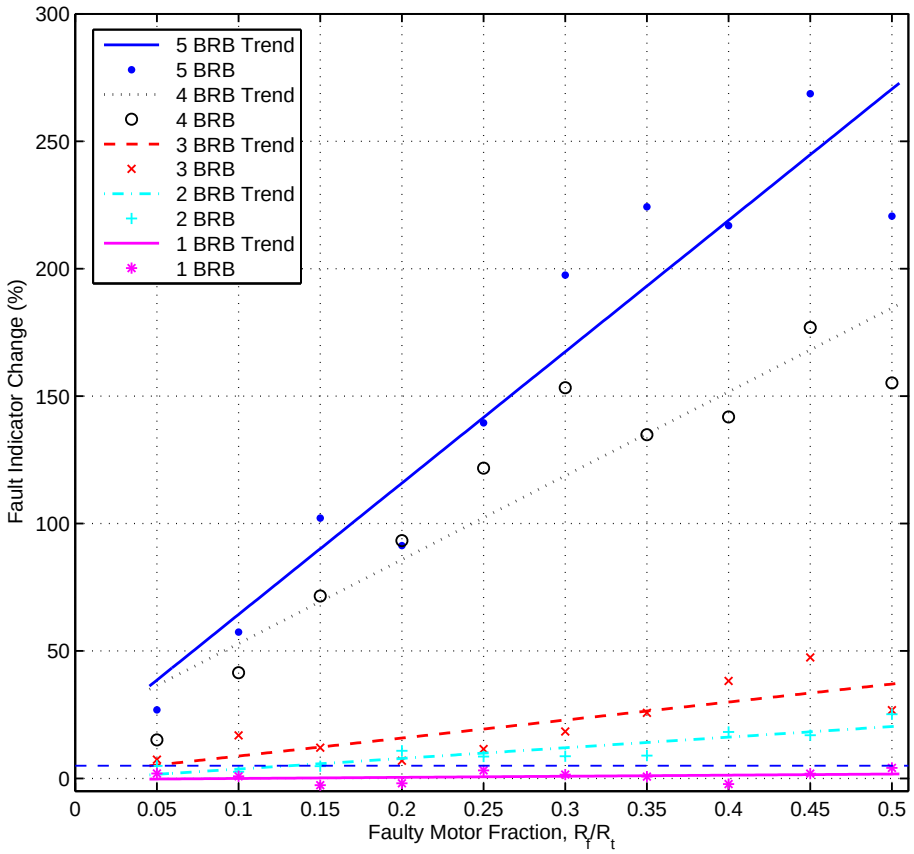

Fig. 25. Variation of Fault Indicator Change, in a configuration of twenty 1 hp 230V motors, with increasing number of faulty motors at different fault severities; configuration specification: $C_{[C,C],[1-10,1-5]}$.

b. 7.5 hp Motor Configuration

Figure 26 shows variation of FIC with increasing number of faulty motors in a configuration of twenty 7.5 hp 460V motors. Up to three broken rotor bars are simulated on the faulty motors, represented by different curves on the plot. Similar to the case of 1 hp motor configuration, the FIC for one broken rotor bar fault on faulty motors did not increase as appreciably as it did in the case of higher fault severities.

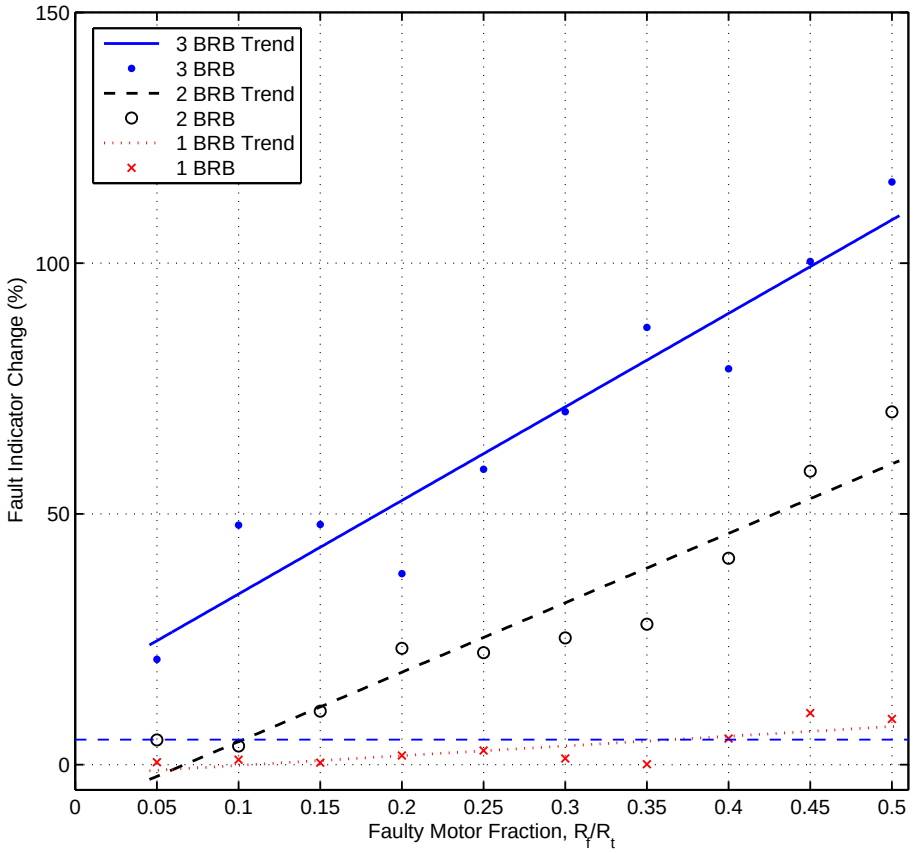

Fig. 26. Variation of Fault Indicator Change, in a configuration of twenty 7.5 hp 230V motors, with increasing number of faulty motors at different fault severities; configuration specification: $C_{[C,C],[1-10,1-3]}$.

G. Discussion of Results

1. Problem A

From the results of Fault Indicator Change analysis of the two motors, viz., 1 hp 460V and 7.5 hp 460V it can be seen that, faults of different fault severities can be easily detected from aggregate currents, even at higher Healthy Motor Fraction. But at values close to one, the fidelity of the indicator drops appreciably and the indicator may fail to detect a fault, irrespective of the fault severity. Hence at higher Healthy Motor Fractions, the ability of the indicator to detect a fault, depends on the variability the healthy indicator is allowed.

The Degradation curves, at different load levels of the configurations, indicate that the load level of the configuration plays an important role in the ability to detect the fault from aggregate measurements. While, an effective increase in the load level on the healthy part of a configuration would make detection difficult, a desired load level for the faulty motor is dictated by the nature of the fault and variation of the faulty motor indicator with the load level [24, 25]. The load level on the faulty motor is not only critical to fault detection from aggregate currents, but may also be exploited for the isolation of the faulty motor, if the variation of faulty motor indicator with the load level is appreciable.

2. Problem B

The results from Problem B suggest that, the individual fault signatures from the faulty motors in a configuration interact differently, depending on the fault severities. While the general trend is of increase in Fault Indicator Change with increasing number of faulty motors, the increase is not appreciable for lower fault severities. Also, the variation is dependent upon the parameters of the individual motors, which

affect the properties of the harmonic components of the faulty and the healthy motors and their manifestation in the aggregate measurements.

H. Chapter Summary

In this chapter, a simulated study of Fault Indicator Change for faults in motor banks, is presented. The simulator used is discussed. Several quantities that are used to present the results are mathematically defined. The problem of study of variation of Fault Indicator Change from aggregate currents, is defined in two forms. The results from the investigation of both the problems are presented.

CHAPTER V

EXPERIMENTAL INVESTIGATION OF FAULT INDICATOR CHANGE IN MOTORS ENERGIZED BY A COMMON VOLTAGE BUS: TWO–MOTOR CONFIGURATION

The aim of the experimental study is to assess the effectiveness of the fault indicator to mechanical faults of different nature and the manifestation of the same in the aggregate currents.

A. Two–Motor Configuration

The experiments are conducted on a 3–phase, 2 pole, 3 hp motor and a 3–phase, 4 pole, 1 hp motor. Both the motors are rated for 208V and are energized by a common voltage bus. The configuration is energized from supply mains, through an auto-transformer. A 8-channel National Instruments data acquisition system is used to collect the voltages and the currents. The experimental setup is depicted in Figure 27

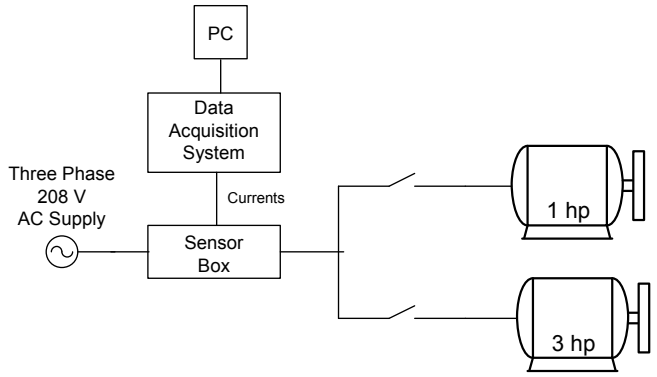

Fig. 27. Two–motor experimental setup.

B. Description of the Experiments Conducted

Experiments with healthy and faulty configurations with differing fault severities, are conducted. While the 1 hp motor is configured for the load eccentricity fault, the 3 hp motor is used to stage the deteriorating bearing faults. Faulty configurations consisted of single or double deteriorating bearing faults on the 3 hp motor and/or eccentric load on the 1 hp motor.

The 3 hp motor used in this work is originally designated to stage the rotor eccentricity experiments and it had an intrinsic 'looseness' of the rotor. The said condition has affected healthy and faulty cases alike. On the 3hp motor, for the single deteriorating bearing cases, bearings are replaced at one end of the rotor (fan end) while maintaining the bearing at the other end (shaft end) healthy. For the double deteriorating bearing cases, the single faulty bearing is maintained at the fan end, the other end is introduced with a faulty bearing.

The two motors are made faulty, alternatively and simultaneously, to stage different faults and fault severities in the configuration. Table IX shows different conditions, the configuration is operated under and the corresponding designations. To study the consistency in results , the rotor of the 3 hp motor is replaced by another compatible rotor and faulty bearing set and the experiments listed are repeated. The two sets of experiments are referred to as case–I and case–II. The healthy experiments of both the motors and faulty experiments of the 3 hp motor are carried out at no-load condition.

The experimental data is obtained at 3840 samples per second and is resampled to 1920 samples per second for the subsequent processing to obtain fault indicators.

Table IX. Different Fault Conditions Staged on the Experimental Configuration and Their Designations

Health Condition			Configuration
S.No.	3 hp with Rotor Looseness	1 hp	Designation
1	Otherwise Healthy	Healthy	Healthy
2	Otherwise Healthy	Load Eccentricity	Fault I
3	Single Deteriorating Bearing	Healthy	Fault II
4	Single Deteriorating Bearing	Load Eccentricity	Fault III
5	Double Deteriorating Bearing	Healthy	Fault IV
6	Double Deteriorating Bearing	Load Eccentricity	Fault V
Note: Two sets of experiments conducted with different rotor and bearing set in 3 hp motor, are referred to as case–I and case–II.			

C. Effectiveness of the Indicator to Different Mechanical Faults

The effectiveness of the indicator developed is tested by calculating the indicator and Fault Indicator Change (FIC) for different faults listed in Table IX, from the individual currents of the motors.

For the 3 hp motor, the Figure 28 shows the indicator magnitudes for the healthy and the faulty cases, and corresponding values of FIC. While the FIC for Fault II is 29.23%, the FIC for Fault IV, is higher at 44.44%. Figure 29 shows the same for the case II, with a different rotor and a different set of faulty bearings in the 3 hp motor. The FIC for Fault II and Fault IV is, 35.71% and 50.94%, respectively.

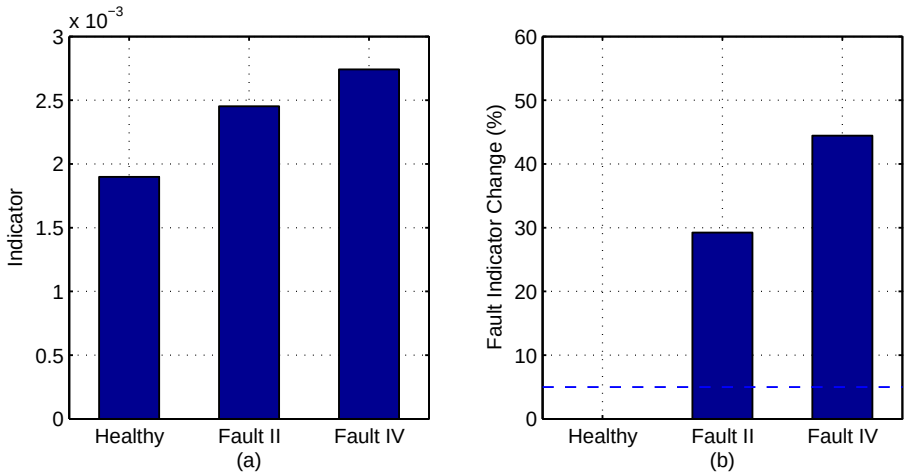

Fig. 28. (a) Indicator value and (b) Fault Indicator Change, for 3 hp motor for the staged faults, case–I.

For the 1 hp motor, Figure 30 shows the indicator magnitudes for the healthy and the faulty case and the corresponding FIC. The FIC for the Fault I is found to be 12.69%.

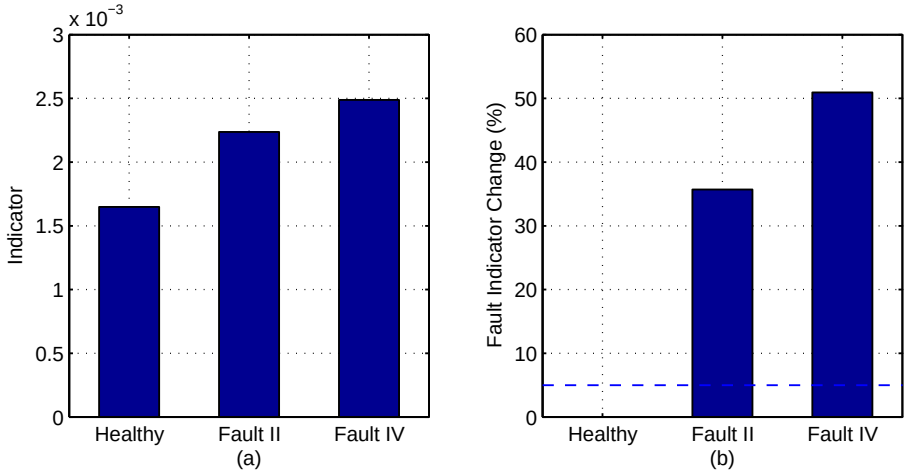

Fig. 29. (a) Indicator value and (b) Fault Indicator Change, for 3 hp motor for the staged faults, case–II.

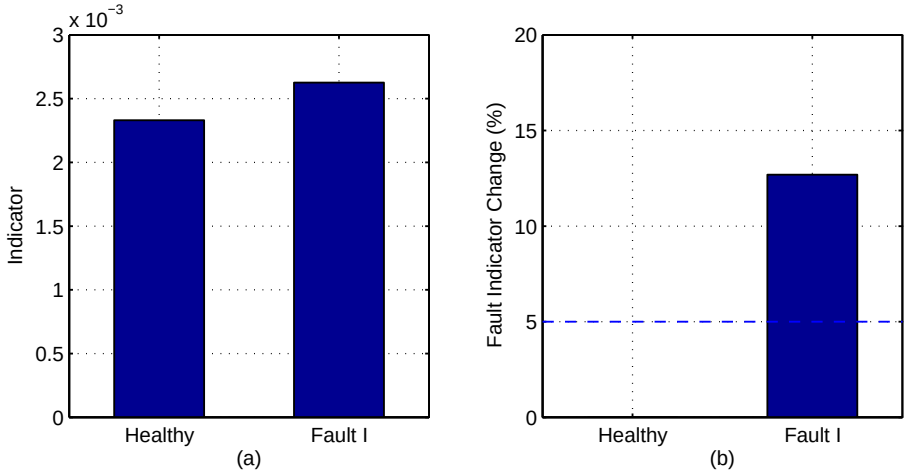

Fig. 30. (a) Indicator value and (b) Fault Indicator Change, for 1 hp motor for the staged fault.

D. Fault Indicator Change from Aggregate Measurements

From the aggregate currents of the configuration, the FIC for faults in either one or both the motors, is calculated. Figure 31 shows the magnitudes of the indicator for different fault conditions listed in Table IX. The FIC for these faults are also shown. The FIC increases steadily with increasing fault severity in the configuration. Figure 32 shows the same for the case II. Tables X, XI list the healthy and faulty indicator magnitudes and the corresponding FIC for both the cases.

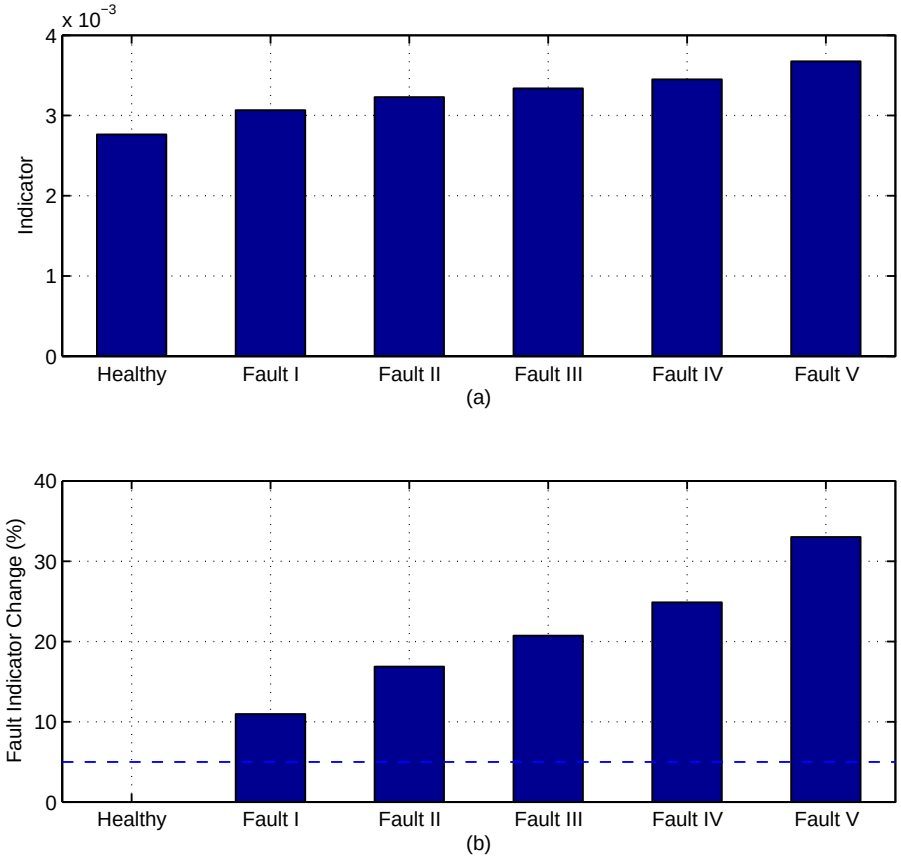

Fig. 31. (a) Indicator value, from the aggregate currents and (b) Fault Indicator Change, for different fault severities in the configuration; case–I.

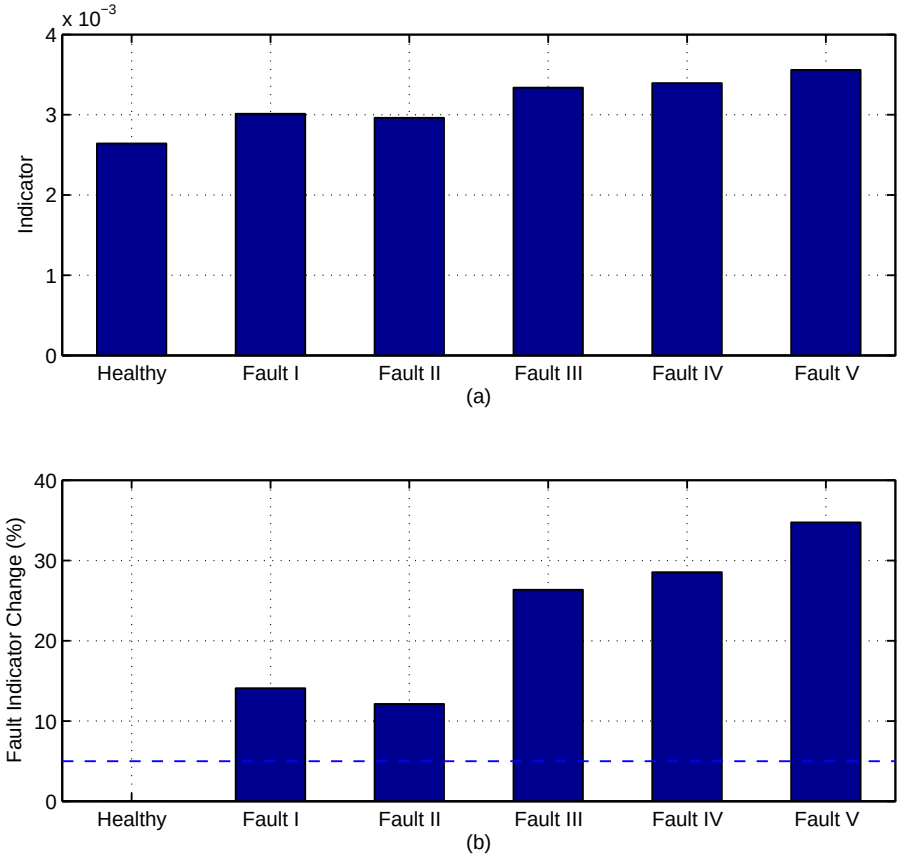

Fig. 32. (a) Indicator value, from the aggregate currents and (b) Fault Indicator Change, for different fault severities in the configuration; case–II.

E. Degradation in Fault Indicator Change from Aggregate Measurements

Degradation can be studied in the configuration, when only one of the two motors is faulty. The faulty motor is made the reference configuration and the FIC from aggregate currents, is compared with the FIC for the faulty motor. Table XI shows the degradation in FIC. Figures 33 and 34 depict the same, for the two cases, in the form of a bar graph along with the FIC from individual and aggregate current

measurements.

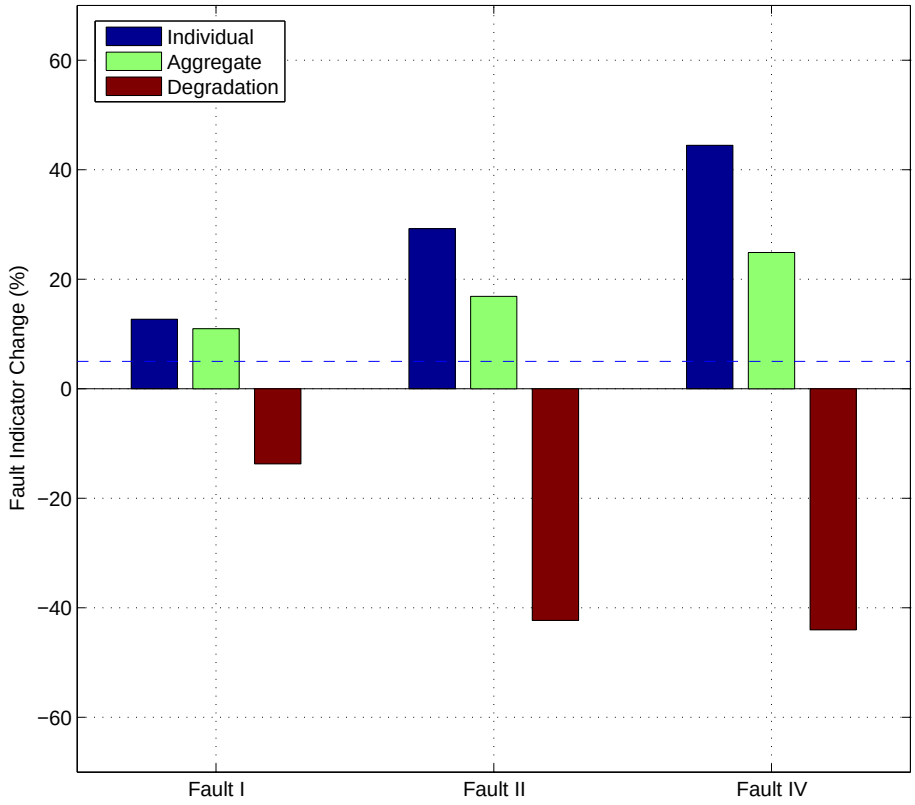

Fig. 33. Fault Indicator Change, from individual currents, aggregate currents and Degradation when using aggregate measurements; case–I.

F. Discussion of Results

Evident from the results presented, the indicator is capable of detecting mechanical faults like, deteriorating bearings in presence of rotor looseness and eccentric load, from the aggregate measurements. The degradation in case of bearing faults is considerable when compared to the same for the eccentric load. Even with considerable

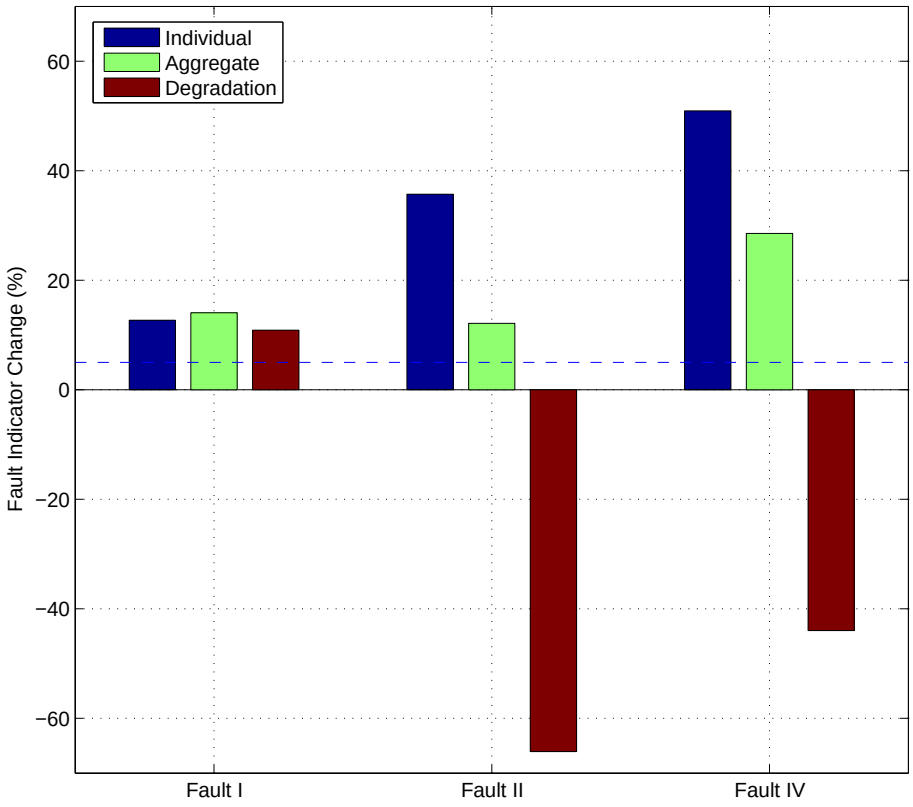

Fig. 34. Fault Indicator Change, from individual currents, aggregate currents and Degradation when using aggregate measurements; case–II.

Table X. Summary of Results from Experimental Study: Indicator Values

Configuration Health Designation	Indicator		
	Individual Measurements		Aggregate Measurements
	3 hp	1 hp	
Case I			
Healthy	0.001898	0.002330	0.002764
Fault I	0.001898	0.002626	0.003067
Fault II	0.002453	0.002330	0.003230
Fault III	0.002453	0.002626	0.003337
Fault IV	0.002742	0.002330	0.003451
Fault V	0.002742	0.002626	0.003676
Case II			
Healthy	0.001648	0.002330	0.002641
Fault I	0.001648	0.002626	0.003013
Fault II	0.002237	0.002330	0.002961
Fault III	0.002237	0.002626	0.003337
Fault IV	0.002488	0.002330	0.003395
Fault V	0.002488	0.002626	0.003559

Table XI. Summary of Results from Experimental Study: Fault Indicator Change and Degradation due to Aggregate Measurements

Configuration Health Designation	FIC (%)			Degradation in FIC (%)
	Individual Measurements		Aggregate Measurements	
	3 hp	1 hp		
Case I				
Healthy	00.00	00.00	00.00	-
Fault I	00.00	12.69	10.95	–13.71
Fault II	29.23	00.00	16.87	–42.28
Fault III	29.23	12.69	20.72	-
Fault IV	44.44	00.00	24.87	–44.03
Fault V	44.44	12.69	33.02	-
Case II				
Healthy	00.00	00.00	00.00	-
Fault I	00.00	12.69	14.07	10.87
Fault II	35.71	00.00	12.12	–66.06
Fault III	35.71	12.69	26.35	-
Fault IV	50.94	00.00	28.54	–43.97
Fault V	50.94	12.69	34.73	-

degradation, a gradual increase in Fault Indicator Change for increasing fault severity shows the effectiveness of indicator in detecting multiple faults, if they occur successively.

G. Chapter Summary

In this chapter, the feasibility of using aggregate currents for detecting faults in a two motor experimental configuration is investigated. The Fault Indicator Change to different faults from individual and aggregate currents, and corresponding degradation, are presented.

CHAPTER VI

SUMMARY AND CONCLUSIONS

A. Summary of Research

The objective of this research is to study the detectability of mechanical faults in induction motors energized by a common voltage bus, using the aggregate bus–level electrical measurements.

In Chapter I, a brief introduction to sensor–less fault detection methods along with common mechanical faults in induction motors is discussed. The existing literature in related areas is reviewed. The objectives of the work and the procedure to be followed is outlined.

In Chapter II, the theory of a detailed model of an induction motor is presented. The state-space representation of the same, used for simulating healthy and faulty motors is also presented.

In Chapter III, the fault indicator employed in this work is developed. The steps involved in extracting the fault indicator from raw currents signals are explained.

In Chapter IV, the simulator used is presented along with the details of the simulations performed. Different quantities used in presentation of results of the chapter, are defined. This chapter presents the analysis of the fault indicator using the aggregate currents obtained from the simulator. Two different problems are defined, to explore the fault indicator in detecting broken rotor bar faults in a motor bank. Problem A, deals with exploring the fault indicator in detecting faults in different configurations having a common faulty motor. The effect of motor load on the detectability of the fault, is studied. Problem B is used to investigate the effects of increasing the number of faulty motors in a given configuration on the aggregate

fault signature. The results from both problems are presented.

In Chapter V, the two–motor experimental configuration is described. The fault indicator is tested for its adaptability to other mechanical faults like, the eccentricity of the load and bearing damage, using the data collected from the experimental test-bed. The Fault Indicator Change from the individual motor measurements and the aggregate measurements, and, degradation in Fault Indicator Change, are presented.

B. Conclusions

From the results and the subsequent discussions presented in the previous two chapters, the following conclusions have been drawn:

- Mechanical faults are detectable from the aggregate measurements of a motor bank.
- Irrespective of the severity of the fault in the faulty motor, the Fault Indicator Change decreases, as the number of healthy motors (amount of healthy horse power) in the motor bank increase. For certain loading conditions, broken rotor bar faults are detectable up to a Healthy Motor Fraction (R_h/R_t) of 0.80.
- The load level of healthy and faulty motors of a configuration affect the Fault Indicator Change. While an increase in load level on the healthy motors degrades the Fault Indicator Change, the desired load level on the faulty motor is dictated by the variation of its fault signature with load.
- In configurations with large number of motors , the Fault Indicator Change is low, when lesser number of motors are faulty, but, it increases as the number of faulty motors increase. Also, single broken rotor bars on multiple motors ($R_f/R_t \leq 0.5$), are not detectable.

- The developed approach is applicable to mechanical faults of different nature like, broken rotor bars, bearing damage with rotor looseness and eccentricity of the load.

C. Future Work

The problem of detecting faults in a motor bank using aggregate electrical measurements is relatively new and presents several prospective research avenues. Some of the topics for future research may include:

- Development of a neuro-predictor capable of predicting the aggregate healthy currents at different load levels of a configuration.
- Detection of the fault and subsequent isolation of the faulty motor in the configuration is very desirable.
- Study of effect of the parameters of motors in a configuration on the aggregate fault signatures.
- A part of the desirable information from the spectrum is lost to the region discarded due to the distortion effects of the notch filtering. Development of signal processing approaches with minimal distortion artefacts may be pursued.

REFERENCES

[1] P. F. Albrecht, J. C. Appiarius, R. M. McCoy, E. L. Owen, and D. K. Sharma, "Assessment of the Reliability of Motors in Utility Applications - Updated," *IEEE Transactions on Energy Conversion*, vol. EC-1, no. 1, pp. 39-46, March 1986.

[2] B. Liang, B. Payne, and A. Ball, "Detection and Diagnosis of Faults in Induction Motors Using Vibration and Phase Current Analysis," *Proceedings of the 1st International Conference on the Integration of Dynamics, Monitoring and Control (DYMAC 99)*, Manchester, UK, pp. 337-341, September 1999.

[3] B. Payne, B. Liang, and A. Ball, "Modern Condition Monitoring Techniques for Electric Machines," *Proceedings of the 1st International Conference on the Integration of Dynamics, Monitoring and Control (DYMAC 99)*, Manchester, UK, pp. 325-330, September 1999.

[4] N. M. Elkasabgy, A. R. Eastham, and G. E. Dawson, "Detection of Broken Bars in the Cage Rotor on an Induction Motor," *IEEE Transactions on Industry Applications*, vol. 28, pp. 165-171, January 1992.

[5] R. R. Schoen, T. G. Habetler, F. Kamran, and R. G. Bartheld, "Motor Bearing Damage Detection Using Stator Current Monitoring," *IEEE Transactions on Industry Applications*, vol. 31, pp. 1274-1279, November/December 1995.

[6] B. Yazici and G. B. Kliman, "An Adaptive Statistical Time-Frequency Method for Detection of Broken Bars and Bearing Faults in Motors Using Stator Current," *IEEE Transactions on Industry Applications*, vol. 35, pp. 442-452, March/April 1999.

[7] W. T. Thomson, D. Rankin, D. G. Dorrell, "On-line Current Monitoring to Diagnose Airgap Eccentricity in Large Three-Phase Induction Motors-Industry Case Histories Verify the Predictions," *IEEE Transactions on Energy Conversions*, vol. 14, no. 4, pp. 1372-1378, December 1999.

[8] K. Kim, "Sensorless Fault Diagnosis of Induction Motors," Ph.D. dissertation, Texas A&M University, College Station, May 2001.

[9] Kim. K., A. G. Parlos, and R. M. Bharadwaj, "Sensorless Fault Diagnosis of Induction Motors," *IEEE Transactions on Industrial Electronics*, vol. 50, No. 5, pp. 1038–1051, 2003.

[10] M. Benbouzid, M. Vieira, C. Theys, "Induction Motors Fault Detection and Localization Using Stator Current Advanced Signal Processing Techniques," *IEEE Transactions on Power Electronics*, vol. 14, no. 1, pp. 14-22, January 1999.

[11] M. Benbouzid, "A Review of Induction Motors Signature Analysis as a Medium for Faults Detection," *IEEE Transactions on Industrial Electronics*, vol. 47, no. 5, pp. 984-993, October 2000.

[12] M. Benbouzid, "Bibliography on Induction Motors Faults Detection and Diagnosis," *IEEE Transactions on Energy Conversion*, vol. 14, no. 4, pp. 1065-1074, December 1999.

[13] G.W. Hart, "Nonintrusive Appliance Load Monitoring," *Proceedings of the IEEE*, pp. 1870–1891, December 1992.

[14] S. B. Leeb, J. L. Kirtley. "A Multiscale Transient Event Detector for Nonintrusive Load Monitoring," *Proceedings of the 1993 IECON International Conference on*

Industrial Electronics, Control and Instrumentation, Maui, Hawaii, pp. 354–359, November 1993.

[15] K. Lee, "Electric Load Information System Based on Non-instrusive Power Monitoring," Ph.D. dissertation, Department of Mechanical Engineering, Massachussetts Institute of Technology, Cambridge, June 2003.

[16] C. D. Salthouse, "Improvements to Non-intrusive Load Monitor," M. Engg. Thesis, Department of Electrical Engineering and Computer Science, Massachussetts Institute of Technology, Cambridge, 2000.

[17] S. R. Shaw, "System Identification Techniques and Modeling for Non-intrusive Load Diagnostics," Ph.D. dissertation, Department of Electrical Engineering and Computer Science, Massachussetts Institute of Technology, Cambridge, January 2000.

[18] K. Matsuse, H. Kawai, Y. Kouno, J. Oikawa, "Characteristics of Speed Sensorless Vector Controlled Dual Induction Motor Drive Connected in Parallel Fed by a Single Inverter," *IEEE Transactions on Industrial Applications*, vol. 40 , no. 1, pp. 153–161, January/February 2004.

[19] Y. Matsumoto, C. Osawa, T. Mizukami, S. Ozaki; "A Stator-Flux-Based Vector Control Method for Parallel-Connected Multiple Induction Motors Fed by a Single Inverter," *Thirteenth Annual Applied Power Electronics Conference and Exposition, APEC '98. Conference Proceedings*, vol. 2 , pp. 575–580, February 1998.

[20] H.A. Toliyat, T.A. Lipo,"Transient Analysis of Cage Induction Machines under Stator, Rotor Bar and End Ring Faults," *IEEE Transactions on Energy Conversion*, volume. 10 , no. 2 , pp. 241–247, June 1995.

[21] H. A. Toliyat, M. S. Arefeen and A. G. Parlos, "A Method for Dynamic Simulation and Detection of Air-Gap Eccentricity in Induction Machines," *IEEE Industry Applications Conference*, vol. 1 , pp. 629–636, 1995.

[22] T. A. Lipo and H. A. Toliyat, "Feasibility Study of a Converter Optimized Induction Motor," *Electric Power Research Institute, EPRI Final Report 2624-02*, Palo Alto, California; January 1989.

[23] H. A. Toliyat, T. A. Lipo and J. C. White, "Analysis of a Concentrated Winding Induction Machine for Adjustable Speed Drive Applications–Part I (Motor Analysis)," *IEEE Transactions on Energy Conversion*, vol. 6, no. 4, pp. 679–684, December 1991.

[24] R. R. Obais and T G. Habetler, "Effect of Load on Detecting Mechanical Faults in Small Induction Motors," *IEEE International Symposium on Diagnosis for Electric Machines, Power Electronics and Drives, SDEMPED 2003*, pp. 307–311, August 2003.

[25] Z. Ye, B. Wu and A. Sadeghian, "Current Signature Analysis of Induction Motor Mechanical Faults by Wavelet Packet Decomposition," *IEEE Transcation on Industrial Electronics*, vol. 50, no. 6, pp. 1217–1228, December 2003.

VITA

Rajesh Kumar Bade, was born in Hyderabad, India. He received his B.E. degree in mechanical engineering from Osmania University, Hyderabad, in 2001. He joined the Department of Mechanical Engineering at Texas A&M University, College Station in January, 2002, to pursue his M.S. degree. He can be reached through, WERC 167, Texas A&M University, College Station, TX, 77843, (979) 845-9650.

The typist for this thesis was Rajesh Kumar Bade.